AMEGHINIANA
A GONDWANAN PALEONTOLOGICAL JOURNAL

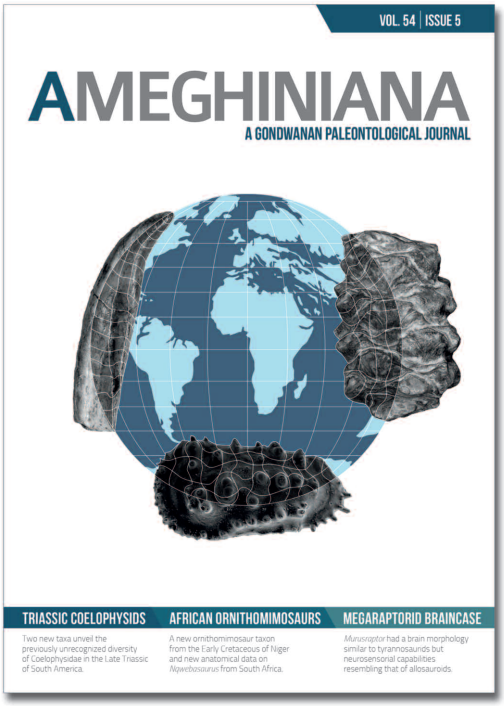

THE BRAINCASE OF THETHEROPOD DINOSAUR *MURUSRAPTOR*: OSTEOLOGY, NEUROANATOMY AND COMMENTS ON THE PALEOBIOLOGICAL IMPLICATIONS OF CERTAIN ENDOCRANIAL FEATURES

ARIANA PAULINA-CARABAJAL[1]
PHILIP J. CURRIE[2]

[1]Instituto de Investigaciones en Biodiversidad y Medioambiente (INIBIOMA), Consejo Nacional de Investigaciones Científicas y Técnicas (CONICET) - Universidad Nacional del Comahue, Quintral 1250, R8400FRF San Carlos de Bariloche, Argentina.
[2]University of Alberta, CW405, Biological Sciences Building, Edmonton, Alberta, Canada.

Submitted: November 7th, 2017 - **Accepted:** March 25th, 2017 - **Published online:** March 28th, 2017

To cite this article: Ariana Paulina-Carabajal, and Philip J. Currie (2017). The braincase of the theropod dinosaur *Murusraptor*: osteology, neuroanatomy and comments on the paleobiological implications of certain endocranial features. *Ameghiniana* 54: 617–640.

To link to this article: http://dx.doi.org/10.5710/AMGH.25.03.2017.3062

Also appearing in this issue:

TRIASSIC COELOPHYSIDS
Two new taxa unveil the previously unrecognized diversity of Coelophysidae in the Late Triassic of South America.

AFRICAN ORNITHOMIMOSAURS
A new ornithomimosaur taxon from the Early Cretaceous of Niger and new anatomical data on *Nqwebasaurus* from South Africa.

MEGARAPTORID BRAINCASE
Murusraptor had a brain morphology similar to tyrannosaurids but neurosensorial capabilities resembling that of allosauroids.

ISSN 0002-7014
AMEGHINIANA - 2017 - Volume 54 (5): 617 – 640
GONDWANAN PERSPECTIVES

THE BRAINCASE OF THE THEROPOD DINOSAUR *MURUSRAPTOR*: OSTEOLOGY, NEUROANATOMY AND COMMENTS ON THE PALEOBIOLOGICAL IMPLICATIONS OF CERTAIN ENDOCRANIAL FEATURES

ARIANA PAULINA-CARABAJAL[1], AND PHILIP J. CURRIE[2]

[1]Instituto de Investigaciones en Biodiversidad y Medioambiente (INIBIOMA), Consejo Nacional de Investigaciones Científicas y Técnicas (CONICET) - Universidad Nacional del Comahue, Quintral 1250, R8400FRF San Carlos de Bariloche, Argentina. *a.paulinacarabajal@conicet.gov.ar*

[2]University of Alberta, CW405, Biological Sciences Building, Edmonton, Alberta, Canada. *philip.currie@ualberta.ca*

Abstract. A detailed description of the neuroanatomy of *Murusraptor barrosaensis*—a mid-sized non-maniraptoran theropod from the Late Cretaceous of north Patagonia—is based on the exceptionally preserved type braincase. CT scans provide new information on the braincase, brain, cranial nerves, encephalic vasculature, and inner ear of this taxon. Worldwide, relatively few non-maniraptoran theropod braincases have been described in detail and the new information reported here is important to better understand the variability of braincase characters within the clade. This study suggests that megaraptorids have a particular brain pattern that is different from those of other non-coelurosaur theropods, such as allosauroids and ceratosaurs, and different from that of some coelurosaurs, such as tyrannosaurids, although sharing more similarities with the latter. The Reptile Encephalization Quotient of *Murusraptor* is within a range between those of *Allosaurus* and *Tyrannosaurus*; the Olfactory Ratio is, however, smaller than the observed in tyrannosaurids and allosauroids. The paleobiological implications on gaze stabilization, hearing, and olfaction in the Argentinean taxon are still poorly understood.

Key words. Maniraptorosaurinae. Neuroanatomy. Inner ear. Olfactory acuity.

Resumen. EL NEUROCRÁNEO DEL DINOSAURIO TERÓPODO *MURUSRAPTOR*: OSTEOLOGÍA, NEUROANATOMÍA Y COMENTARIOS SOBRE LAS IMPLICANCIAS PALEOBIOLÓGICAS DE ALGUNOS CARACTERES ENDOCRANEANOS. Una descripción detallada de la neuroanatomía de *Murusraptor barrosaensis*—un terópodo no-maniraptoriforme de tamaño mediano del Cretácico Superior de Norpatagonia—se presenta aquí, basada en el neurocráneo excepcionalmente preservado del holotipo. Las tomografías computadas brindaron nueva información sobre el neurocráneo, encéfalo, nervios craneanos, vasculatura y oído interno de este taxón. Relativamente pocos neurocráneos de terópodos no-coelurosaurios han sido descritos en detalle a nivel mundial, y la nueva información osteológica reportada aquí es importante para entender mejor la variabilidad de los caracteres neurocraneanos en el clado, sugiriendo también que los megaraptóridos tendrían un patrón morfológico endocraneano que difiere de otros terópodos no-coelurosaurios tales como ceratosaurios y allosauroideos, y de coelurosaurios no-maniraptores como los tiranosáuridos (si bien, compartiendo más similitud con éstos últimos). El Coeficiente de Encefalización Reptiliano de *Murusraptor* se encuentra en un rango entre el de *Allosaurus* y *Tyrannosaurus*; mientras que el Cociente Olfatorio es menor que el calculado para tiranosáuridos y allosauroideos. Las implicancias paleobiológicas sobre estabilización visual, audición y olfato para este taxón argentino, son aún poco comprendidas.

Palabras clave. Maniraptorosaurinae. Neuroanatomía. Oído interno. Capacidad olfatoria.

MURUSRAPTOR BARROSAENSIS Coria and Currie, 2016 is a megaraptoran theropod from the Sierra Barrosa Formation (Turonian–Coniacian; Garrido, 2010), Late Cretaceous of northern Patagonia (Coria and Currie, 2016). Megaraptorids are non-maniraptoran theropods (Novas, 1998, 2009) with controversial phylogenetic relationships that have been either considered as members of the Allosauroidea—closely related to carcharodontosaurids and allosaurids (Benson *et al.*, 2010; Carrano *et al.*, 2012; Coria and Currie, 2016)—or Coelosauroidea (Novas *et al.*, 2013; Porfiri *et al.*, 2014). The type specimen of *Murusraptor* was recovered with an exceptionally well preserved braincase, which was isolated from the rest of the preserved skull bones (Figs. 1–3, S1).

The presence of sutures between most of the elements of the braincase of *Murusraptor* permitted the digital modeling and virtual separation of most bones, allowing the observation of internal and external surfaces (Figs. S2–S6). Exceptions were bones that fuse early during the ontogeny, such

as the basisphenoid-parasphenoid, epiotic-supraoccipital, exoccipital-opisthotic (Currie, 1997), and orbitosphenoid-laterosphenoid, the contacts of which were poorly visible in the CT scans. Although the knowledge of braincase anatomy of non-coelurosaur theropods has increased dramatically in the past 20 years (*e.g.*, Currie and Zhao, 1993a, b; Coria and Currie, 2002a; Rauhut, 2004; Franzosa and Rowe, 2005; Ezcurra, 2007; Sampson and Witmer, 2007; Paulina-Carabajal, 2009, 2011a, b, 2015; Cau *et al.*, 2012; Paulina-Carabajal and Currie, 2012; Porfiri *et al.*, 2014; Xing *et al.*, 2014; Filippi *et al.*, 2016), most braincase descriptions do not include endocranial features (or at best only a few of them). The availability of CT scanners, working in conjunction with computer hardware and software, has allowed such studies in recent years. Particularly in terms of endocranial morphology, few Cretaceous non-maniraptoran theropods have been studied. These mostly include allosauroids, such as *Acrocanthosaurus* (Franzosa and Rowe, 2005), *Carcharodontosaurus* (Larsson *et al.*, 2000; Larsson, 2001), and *Giganotosaurus* (Paulina-Carabajal and Canale, 2010), and abelisaurids, such as *Majungasaurus* (Sampson and Witmer, 2007), *Aucasaurus* (Paulina-Carabajal, 2011a; Paulina-Carabajal and Succar, 2015) and *Viavenator* (Paulina-Carabajal and Filippi, 2016). The endocranial morphology of Jurassic theropods is known for *Coelophysis rhodesiensis* (= *Syntarsus*, unpublished thesis of Raath, 1977), *Ceratosaurus* (Sanders and Smith, 2005), *Sinosaurus* (Xing *et al.*, 2014), and the allosauroids *Allosaurus* (Rogers 1998, 1999; Franzosa, 2004) and *Sinraptor* (Paulina-Carabajal and Currie, 2012). Finally, there are only preliminary studies or illustrations of the endocranial morphology of Triassic theropods such as *Herrerasaurus* (Dufeau, 2011: fig. 1.10.B) and *Zupaysaurus* (Paulina-Carabajal *et al.*, 2015b).

This paper focuses on the holotype braincase of *Murusraptor*, which represents the most complete megaraptorid braincase known so far. Within Megaraptoridae, a partially preserved braincase is known for a juvenile specimen referred to *Megaraptor namunhuaiquii* (Novas, 1998; Porfiri *et al.*, 2014). An isolated theropod frontal from the Late Cretaceous of northern Patagonia (Paulina-Carabajal and Coria, 2015) exhibits some features shared with *Murusraptor*, and probably represents a related form.

The CT scans of the braincase of *Murusraptor* allowed the reconstruction of the cranial endocast, inner ear and pneumatic cavities, adding important new morphological data to the knowledge of this species. The cranial endocast of *Murusraptor* is complete and several morphological features can be recognized in the forebrain, midbrain, and hindbrain regions. The inner ear of *Murusraptor* is also reconstructed and compared with the inner ears of other theropods. Furthermore, the acuity of some senses, such as olfaction and hearing, can now be evaluated more accurately. Consequent paleobiological implications are considered based on inner ear morphology, and on calculations of the Reptile Encephalazation Quotient (Jerison, 1973; Hurlburt, 1996) and the Olfactory Ratio (Zelenitsky *et al.*, 2009). The new information on the endocranial morphology and inner ear of *Murusraptor* represents important data to better understand the evolutionary patterns of brain morphology within Theropoda.

MATERIAL AND METHODS

The braincase morphology of *Murusraptor* was described previously (unpublished Doctoral Thesis of Paulina-Carabajal, 2009; Coria and Currie, 2016). Therefore, the description in this paper focuses on newly observed anatomical details,

Figure 1. 1–8, Photographs (left column) and line-drawings (right column) of the braincase of ***Murusraptor*** (**MCF-PVPH** 411). **1–2,** dorsal view; **3–4,** right lateral view; **5–6,** ventral view; **7–8,** posterior view. Abbreviations: **bo,** basioccipital; **bs,** basisphenoid; **bsr,** basisphenoidal recess; **bt,** basal tuber; **btp,** basipterygoid process; **btr,** basipterygoid recess; **cmcv,** caudal middle cerebral vein foramen; **col,** columellar recess; **cul,** cultriform process; **eo,** exoccipital; **f,** frontal; **fm,** foramen magnum; **f-p.su,** frontoparietal suture; **ic,** internal carotid artery foramen; **if.su,** interfrontal suture; **ip.su,** interparietal suture; **ls,** laterosphenoid; **ltr,** lateral tympanic recess; **nas.f,** nasal process of frontal; **nc,** nuchal crest; **oc,** occipital condyle; **ocv,** orbitocerebral vein; **op,** opisthotic; **os,** orbitosphenoid; **p,** parietal; **pa,** parietal ala; **pf.sc,** surface of contact with prefrontal bone; **pn,** pneumatic foramina; **po.f,** postorbital process of frontal; **po.ls,** postorbital process of laterosphenoid; **pop,** paroccipital process; **pp,** preotic pendant; **pro,** prootic; **scr,** subcondylar recess; **so,** supraoccipital; **so.k,** supraoccipital knob; **stf.m,** anterior margin of supratemporal fossa; **I–XII,** cranial nerve foramina; **V_1,** ophthalmic branch of trigeminal nerve; **$V_{2,3}$,** maxillomandibular branches of trigeminal nerve; **IX_{tv},** tympanic branch of glossopharyngeal nerve?; **1,** probable tooth mark?; **2,** pit and triangular projection dorsal to the postorbital process of frontal (after Paulina-Carabajal, 2009). Scale bar= 50 mm.

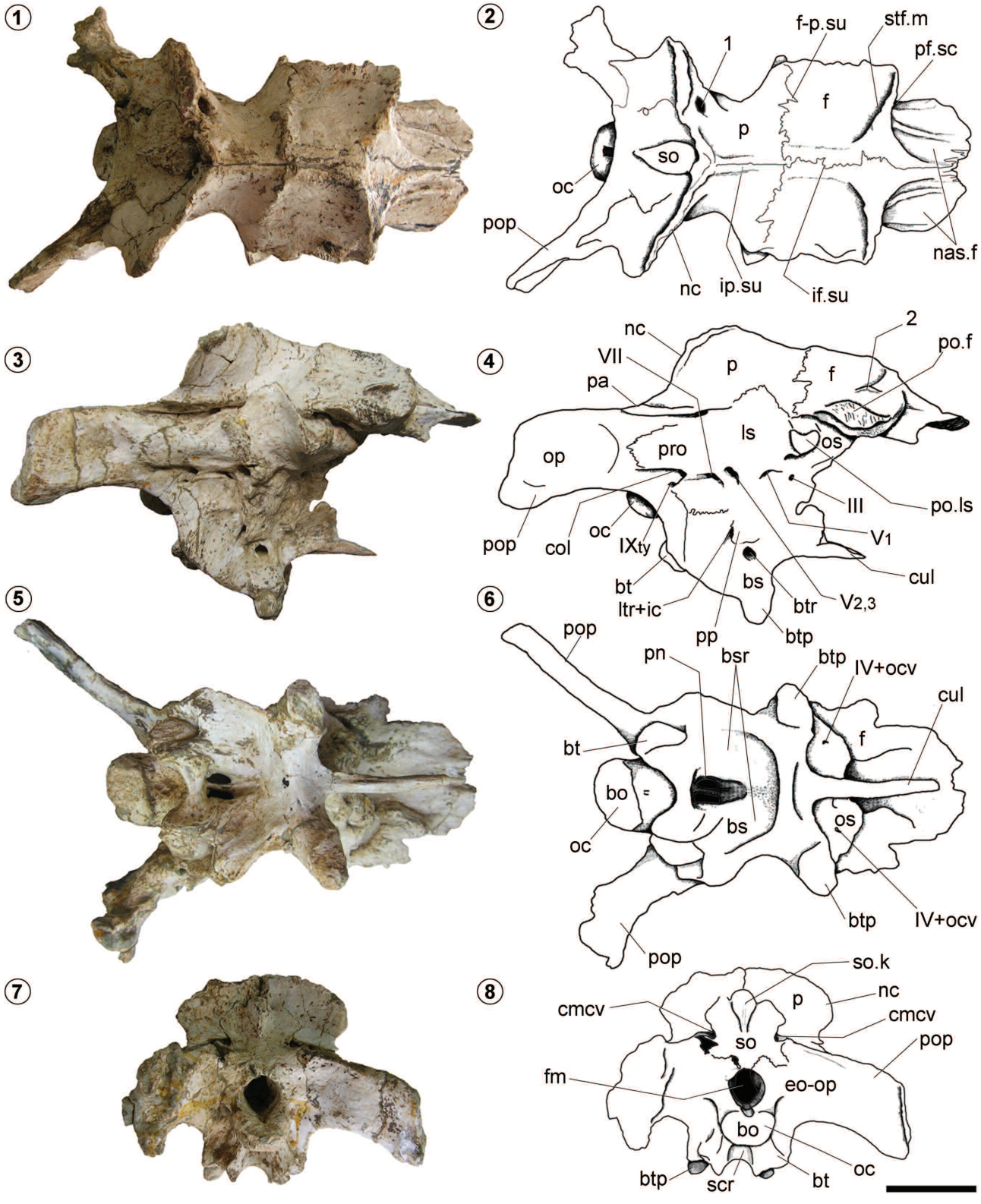
1
2
f-p.su
stf.m
pf.sc
1
f
p
so
oc
pop
nc
ip.su
if.su
nas.f
3
4
nc
2
po.f
VII
p
f
pa
ls
os
op
pro
III
po.ls
pop
col
oc
IXty
V1
cul
bt
ltr+ic
bs
btr
V2,3
5
6
pop
pn
bsr
btp
IV+ocv
cul
pp
btp
bt
f
bo
os
oc
bs
btp
IV+ocv
pop
7
8
so.k
p
nc
cmcv
cmcv
so
pop
fm
eo-op
bo
oc
btp
scr
bt

and on cranial neurovascular foramina, sutures, and those aspects that were revealed by CT scans of the endocranial cavity, the inner ear, and pneumatic cavities.

The sediment infilling the endocranial cavity and pneumatic recesses of the braincase of *Murusraptor* was mechanically removed by the first author to obtain better CT scanning contrast (Paulina-Carabajal, 2009).

The brain morphology of *Murusraptor* was studied using a digital cranial endocast based on CT scans. Because the sphenethmoids (enclosing the olfactory bulbs) are separate, a latex endocast of the olfactory bulb cavity was also made to allow the calculation of the complete cranial endocast volume. The X-ray CT scan of the type specimen was made on June 8, 2004 at the Foothills Hospital, Calgary (Alberta, Canada), using a medical tomographer (model GE LightSpeed QX/i). Slices were taken at intervals of 1.5 mm, with an overlap of 0.63 mm. The braincase was scanned in two positions that produced 415 coronal slices and 299 sagittal slices. The gray scale values were clear enough to differentiate all the structures mentioned. The digital reconstructions of the cranial endocast and inner ear were made using the software Materialise Mimics (14.0 and 18.0, automatic thresholding). Final images for publication were made using Adobe Photoshop (CS3).

As mentioned by other authors (Jerison, 1973; Hopson, 1979; Evans, 2005; Balanoff *et al.*, 2010), most dinosaur cranial endocasts do not precisely reproduce the shapes of the brains (soft tissues). They show the morphologies of the endocranial spaces, which represent structures such as meninges and venous sinuses. However, they can be used to approximate structures of the brain. As proposed by Witmer *et al.* (2008), the digital casts of structures will be referred to as if they are the structures themselves (for example, ''olfactory bulb'' will be used instead of ''endocast of olfactory bulb cavity") to facilitate discussion in the text.

Body mass calculation

The body mass of *Murusraptor* was calculated as the first step in the calculation of the Reptile Encephalization Quotient (**REQ**). Because there is no preserved femur for this taxon, the body mass was inferred comparing the length and width measurements of the tibia of *Murusraptor*, with the tibiae measurements and body masses calculated by Christiansen and Fariña (2004) for the allosauroid theropods *Allosaurus* and *Sinraptor*. The result is an inferred body mass for *Murusraptor* of approximately 1465–1578 kg. The average of 1521 kg was used to calculate the REQ (using the maximum and minimum values does not significantly affect the results presented here).

Encephalazation Quotient calculation

A commonly used measure of relative brain size within theropods is the Encephalization Quotient (**EQ**; Jerison, 1973). Hurlburt (1996) developed the Reptile Encephalization Quotient (REQ), using equations based on extant reptile species. Following Hurlburt *et al.* (2013), the REQ of *Murusraptor* was calculated using the following equation: REQ= MBr/ (0.0155 × $MBd^{0.553}$), where **MBr** is the brain mass and **MBd** is the body mass (Tab. 1). The methods for calculating the brain (endocranial cast) volume are based on CT scans for *Murusraptor*, *Giganotosaurus*, and *Sinraptor* (Paulina-Carabajal and Currie, 2012; Paulina-Carabajal *et al.*, 2015a). However, the volume of the brain of *Carcharodontosaurus* was calculated by Larsson (2001) using Double Graphic Integration.

The volume of the digital cranial endocast of *Murusraptor* (excluding the olfactory bulbs) was calculated with tools of the software Mimics, and is approximately 141.2 cm^3. The volume of the olfactory bulbs was calculated by water displacement from a latex cast of the cavity enclosed within the isolated sphenethmoids (which are separate from the rest of the braincase and not included in the CT scans) and is approximately 7 cm^3 (Fig. 3).

Olfactory ratios

Olfactory ratios (see Zelenitsky *et al.*, 2009 and references therein) can be used to interpret the olfactory acuity in extinct animals. The olfactory ratio in *Murusraptor* was calculated as the ratio between the greatest diameter of the olfactory bulb (measured from the dorsal view of the digital cranial endocast and from the impression left on the ventral side of the frontals) and the longest diameter of the cerebral hemisphere (measured from the cerebral hemisphere region of the cranial endocast), regardless of orientation, and multiplied by 100 (see Zelenitsky *et al.*, 2009, 2011 for methodology).

TABLE 1 – Endocranial values, Reptile Encephalization Quotient and Olfactory Ratios of* Murusraptor *compared to other theropods.

Taxon	*EV (ml)*	*Mbr (ml) 37%*	*Mbr (ml) 50%*	*Mbd (kg)*	*REQ 37%*	*REQ 50%*	*REQ 100%*	*OR 50%*	*asc-psc angle*
Murusraptor	*148.2*	*54.8*	*74.1*	*1551*	*1.33*	*1.8*	*3.6*	*45–50*	*~80*
MCF-PVPH 320	-	-	-	-	-	-	-	*~45*	-
Giganotosaurus	*275* [4]	*101.7*	*137.5*	*7000* [1]	*1.07*	*1.4*	*2.9*	*50–57* [5]	*~67* [8]
Carcharodontosaurus	*263.6* [3]	*97.5* [3]	*131.8* [3]	*7000* [3]	*1.03* [3]	*1.4* [3]	-	*56* [5]	-
Sinraptor dongi	*95.0*	*35.1*	*47.5*	*1700* [2]	*0.81*	*1.1*	*2.19*	*55* [6]	*~65* [6]
Allosaurus[4]	*169–188*	*62.5–69.5*	*84.5–93.9*	*1400–2300*	*1.3–1.8*	*1.8–2.4*	*3.28*	*~50* [5]	*~80*
Majungasaurus	*106.4* [7]	*39.4*	*53.2* [7]	*1130* [7]	*1.14*	*1.54*	*3.08*	*48.3* [5]	*~85*
Tyrannosaurus[4]	*414.2*	*153.2*	*207.1*	*5654–7000*	*1.8–1.6*	*2.5–2.2*	*4.4–4.9*	*66–71* [5]	-

[1]Mazzetta et al. *(2004); [2]Christiansen and Fariña (2004); [3]Hurlburt* et al. *(2013); [4]Paulina-Carabajal and Canale (2010); [5]Zelenitsky* et al. *(2009); [6]Paulina-Carabajal and Currie (2012); [7]Sampson and Witmer (2007); [8]Paulina-Carabajal* et al. *(2015a).*
Abbreviations: ***asc/psc,*** *angle formed between the anterior and posterior semicircular canals of the inner ear in dorsal view;* ***EV,*** *endocranial volume;* ***Mbd,*** *body mass;* ***Mbr,*** *brain volume;* ***OR,*** *olfactory ratio (see Zelenitsky* et al., *2009);* ***REQ,*** *Reptile Encephalization Quotient, 37–100% values represents minimum and maximum estimated occupation of the endocranial cavity (see Hurlburt* et al., *2013).*

Supplementary information

An interactive 3D PDF of the surface models of the braincase, brain and inner ear of *Murusraptor* was made using the software Geomagic (Fig. S1). Using the software Mimics, different bones of the braincase (or regions of fused elements of the braincase) were segmented individually and painted in different colors following the observed sutural contacts. Each bone could be virtually separated and reconstructed three-dimensionally as isolated components, including the basicranium (basioccipital-basisphenoid-parasphenoid), exoccipital-opisthotic, laterosphenoid-laterosphenoid, prootic, and supraoccipital (Figs. S2–S6). Furthermore, the pneumatic cavities (basisphenoidal recess, basipterygoid recess and lateral tympanic recess) were reconstructed in different colors in selected sets of coronal slices of the braincase (Figs. S7–S9).

***Institutional Abbreviations*.** **BMNH,** The Natural History Museum, London, United Kingdom; **IVPP,** Institute of Vertebrate Paleontology and Paleoanthropology, Beijing, China; **LACM,** Los Angeles County Museum, Los Angeles, USA; **MACN,** Museo Argentino de Ciencias Naturales "Bernardino Rivadavia", Buenos Aires, Argentina; **MAU,** Museo Argentino Urquiza, Rincón de los Sauces, Argentina; **MCF,** Museo "Carmen Funes", Plaza Huincul, Argentina; **MNHN,** Muséum National d'Histoire Naturelle, París, France; **MUCPV,** Museo de la Universidad Nacional del Comahue, Centro Paleontológico Lago Barreales, Neuquén, Argentina; **MUCPV-CH,** Museo de la Universidad Nacional del Comahue, El Chocón, Argentina; **PVL,** Paleontología de Vertebrados Lillo, Universidad Nacional de Tucumán, San Miguel de Tucumán, Argentina; **PVSJ,** Museo de la Universidad Nacional de San Juan, San Juan, Argentina; **SGM,** Ministére de l'Energie et des Mines, Rabat, Morocco; **SMNS,** Staatliches Museum für Naturkunde, Stuttgart, Germany; **TMP,** Royal Tyrrell Museum of Palaeontology, Drumheller, Canada; **USNM,** National Museum of Natural History, Smithsonian Institution, Washington, USA; **UUVP,** University of Utah, Salt Lake City, USA.

DESCRIPTION

Braincase

The braincase of *Murusraptor* (MCF-PVPH 411) is complete (Paulina-Carabajal, 2009; Coria and Currie, 2016), three-dimensionally preserved, and shows no diagenetic deformation. There is, however, marked bilateral asymmetry produced by an injury (infection or disease, probably fatal in time) occurred during the animal's lifetime (Fig. 1). The paleopathological ailment on the left side of the braincase

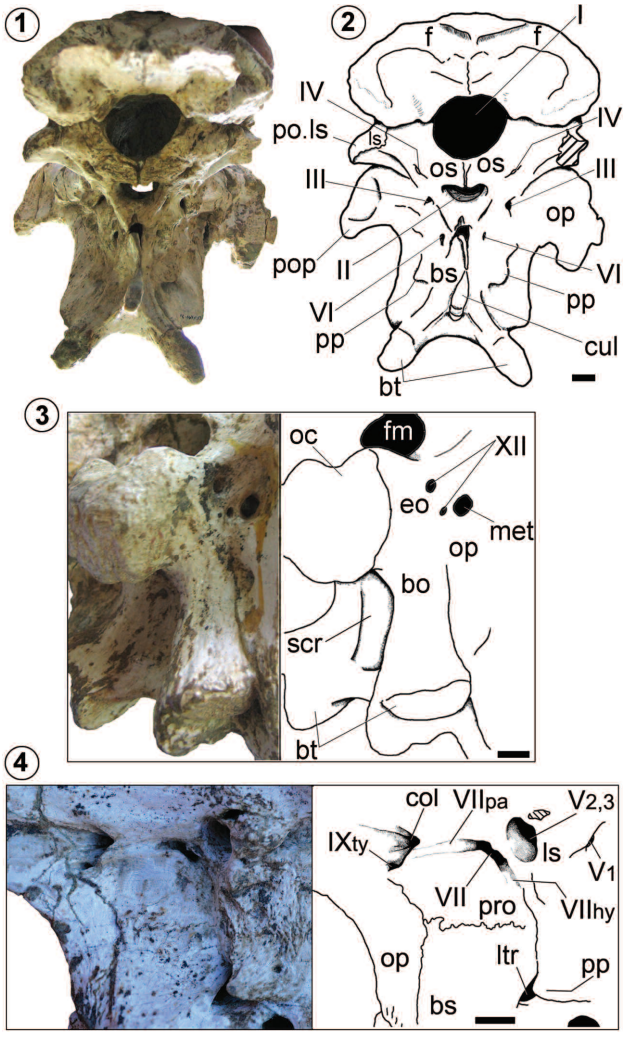

Figure 2. Photographs (left) and line-drawings (right) of the braincase of ***Murusraptor*** **(MCF-PVPH** 411). **1–2,** anterior view; **3,** right posterolateral view of basicranium (detail of cranial nerve foramina); **4,** lateral view, detail of prootic and laterosphenoid, and neurovascular foramina. Abbreviations as in Figure 1: **met,** metotic foramen (for CNs IX–XI); **VII_{hy},** hyomandibular branch of facial nerve; **VII_{pa},** palatine branch of facial nerve (after Paulina-Carabajal, 2009). Scale bars= 10 mm.

affected particularly the endochondral bones and the left half of the nuchal crest (Figs. 1, S1). The nuchal crest has an expanded dorsal margin with two irregular openings on the anterior side that connect internally with a single irregular cavity. Those two pits were interpreted as remnants of tooth marks (Coria and Currie, 2016). However, the reabsorption and remodeling of the margins of these openings would have eliminated details such as marks left by tooth serrations (Fig. 1.1). Differences between left and right sides of the braincase are restricted to measurements, shapes, and textures of the surfaces of the bones (see Fig. S1). There are also differences in the sizes, shapes, and relative distribution of the neurovascular foramina (cranial foramina IX–XII), which are larger and have irregular margins on the pathological side. The injury also affected the development of the internal pneumatic cavities (Paulina-Carabajal, 2009). The identification of the nature of this pathology (*e.g.*, metastasis, exostosis, presence of tumors, or osteomyelitis) is not the primary objective of this paper. However, it is evident from the degree of bone reabsorption and remodeling that the animal survived a certain period of time with this affection, although the injury may have been serious enough to have ultimately caused the death of this individual.

The braincase of *Murusraptor* is anteroposteriorly short and tall. The occipitofrontal angle (Coria and Currie, 2002a), measured between the skull roof and the plane formed by the foramen magnum and the basal tubera is acute (approximately 65°) (Fig. 4), being similar to the angles seen in abelisaurids (60°). This contrasts with the obtuse angles observed in the braincases of *Ceratosaurus* (98°; Sanders and Smith, 2005), carcharodontosaurids, and sinraptorids (Coria and Currie, 2002a: fig. 6A–C). Sanders and Smith (2005) stated that the obtuse occipitofrontal angle of the braincase and relatively unflexed shape of the endocranium in *Ceratosaurus* indicate a horizontal craniocervical posture. Although these anatomic relationships have yet to be determined in other theropods, this suggests that *Murusraptor* had a more anteroventrally craniocervical posture (with the skull inclined anteroventrally).

Skull roof. The parietals are anteroposteriorly short compared to the frontal length (Figs. 5.1, S3). The parietals are not fused along the midline, and the interparietal suture is clearly visible dorsally (Fig. 1.1). This is unlike the conditions of most theropods in which the parietals fuse into a single, unpaired element during early ontogenetic stages (Currie, 1997). The presence of visible sutures in the braincase indicates that the specimen represents a subadult animal (Paulina-Carabajal, 2009; Coria and Currie, 2016). However, the presence of the interparietal suture (which closes early during ontogeny in most theropods) on the skull roof may have phylogenetic implications.

The sinuous frontoparietal suture is mainly transverse to the axial plane. It is thickened prominently above the su-

ture near the midline (Fig. 5.1). This thickened suture protrudes into the supratemporal fossa, possibly indicating the separation of two muscle bodies (Paulina-Carabajal, 2009), corresponding to the *m. pseudotemporalis superficialis* anteriorly and the *m. adductor mandibulae profundus* posteriorly (Holliday, 2009). A similar thickened suture is also observed in *Acrocanthosaurus* (Currie and Carpenter, 2000), *Giganotosaurus* (MUCPV-CH-1), and *Sinraptor* (IVPP 10600; Currie and Zhao, 1993a). Ventrally (endocranially), the frontoparietal suture is not transverse, but an anteromedial, triangular projection of the parietals separates the frontals posteroventrally (Fig. 5.2). This trait is the opposite of that seen in the isolated theropod frontal from the Late Cretaceous of Patagonia MCF-PVPH 320 (Paulina-Carabajal and Coria, 2015) and in *Piatnitzkysaurus* (PVL 4073; Paulina-Carabajal, 2009). In each of these animals, there is an anterodorsal medial process of the parietal separating the frontals posteriorly, whereas the ventral frontoparietal contact is transverse (Fig. 5.5–6). Tyrannosaurids in turn, have parietals forming an anterior projection that separates the frontals posteriorly for their complete height (resulting in a V-shaped frontoparietal suture both, dorsally and ventrally (Paulina-Carabajal, 2009) (Fig. 5.3–4). The presence of this dorsal median projection of the parietals separating the frontals posteriorly seems to be of phylogenetic importance (*e.g.*, Currie *et al.*, 2003).

The frontals are the most conspicuous elements in the skull roof. Their dorsal surfaces are not flat, but markedly lateroventrally inclined, leaving a blunt sagittal bar that is 6 mm wide. The lateroventral inclination of the frontal probably corresponds to an enlargement of the insertion surface of the temporal bones (Paulina-Carabajal, 2009).

On the ventral surfaces of the frontals, there are shallow olfactory tract and olfactory bulb impressions (Figs. 5.2, 6.2). Lateral to each olfactory bulb impression there is a small, semilunate longitudinal concave depression that indicates the contact with the sphenethmoid (Paulina-Carabajal, 2009; Coria and Currie, 2016) (Fig. 5.2). The sphenethmoids of *Murusraptor* are U-shaped and, therefore, the frontals form the roof of the cavities occupied by the olfactory bulbs and olfactory tracts (Fig. 3), unlike abelisaurids, carcharodontosaurids, and tyrannosaurids (Ali *et al.*, 2008; Paulina-Carabajal and Currie, 2012), which have sphenethmoids that encircle the olfactory bulbs and tracts (at least anteriorly) and exclude the frontals form the roof of the cavity. When the sphenethmoids of *Murusraptor* are in natural anatomical position, there remains a hiatus of approximately 10 mm between the anterior margin of the orbitosphenoids and the posterior margin of the sphenethmoids, which corresponds to an unossified section of the ethmoidal elements. The same hiatus is present in the allosauroid *Sinraptor*, and probably represents a cartilaginous section of the sphenethmoids, or a different ossification, such as the septosphenoid (Paulina-Carabajal, 2009; Paulina-Carabajal and Currie, 2012: fig. 8).

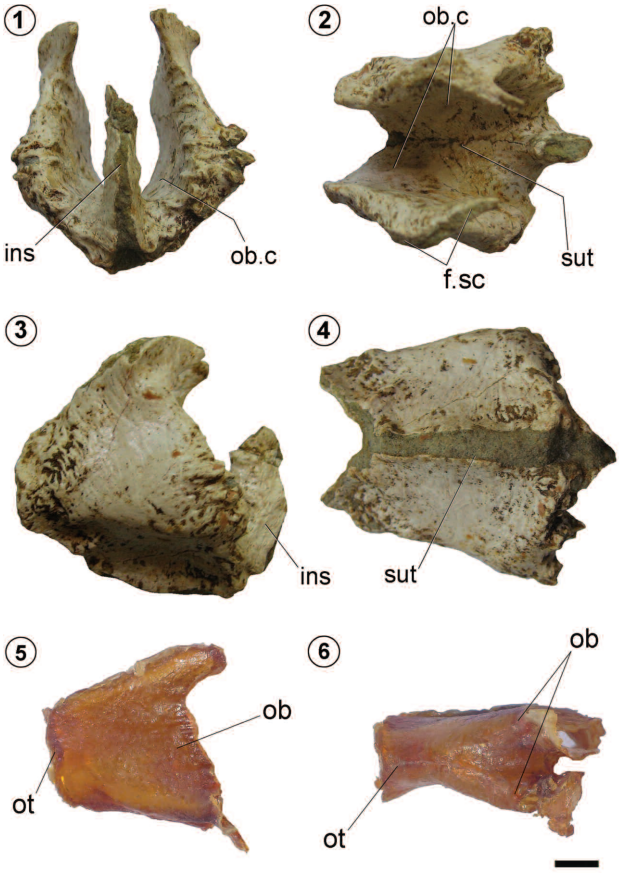

Figure 3. 1–4, Photographs of the ossified ethmoidal elements of ***Murusraptor*** **(MCF-VPH** 411); **1,** anterior view; **2,** dorsal view; **3,** right lateral view; **4,** ventral view; **5–6,** Photographs of the latex endocast of the olfactory bulb cavities and anterior region of the olfactory tract; **5,** right lateral view; **6,** ventral view. Abbreviations: **ins,** internasal septum formed by mesethmoids?; **f.sc,** surface of contact with the frontal; **ob,** olfactory bulb; **ob.c,** olfactory bulb cavity; **ot,** olfactory tract; **sut,** suture. Scale bar= 10mm.

Supraoccipital. The supraoccipital is not on the same vertical

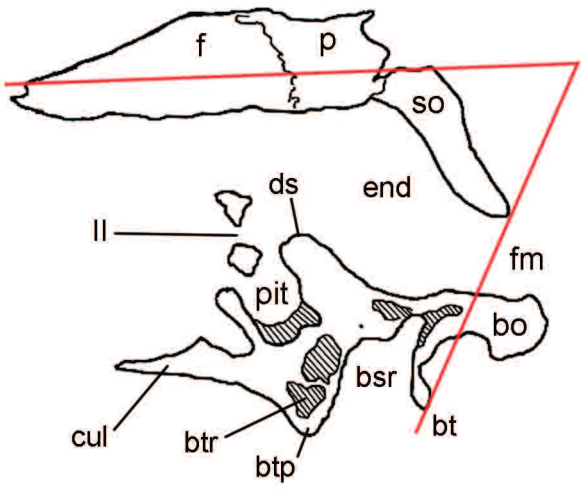

Figure 4. Schematic based on a sagittal section (CT scan) of the braincase of ***Murusraptor*** (**MCF-PVPH** 411) showing the occipitofrontal angle and some endocranial structures. Abbreviations: **bo,** basioccipital; **bsr,** basisphenoid recess; **bt,** basal tuber; **btp,** basipterygoid process; **btr,** basipterygoid recess; **cul,** cultriform process; **ds,** dorsum sellae; **end,** endocranial cavity; **f,** frontal; **fm,** foramen magnum; **p,** parietal; **pit,** pituitary fossa; **so,** supraoccipital; **II,** cranial nerve (after Paulina-Carabajal, 2009). Not to scale.

plane as the exoccipitals, but anterodorsally inclined, forming a wide angle between the vertical occiput and the horizontal skull roof (Fig. 4). The supraoccipital knob is a teardrop-shaped protuberance developed on the dorsal half of the element (Fig. 1.7). On the dorsal surface of the braincase, between the supraoccipital and the parietal, there is a small unossified region along the midline, probably occupied by cartilage, due the stage of immaturity of the specimen. On the posterior surface of the occiput, on each side of the supraoccipital and delimited laterally by the parietal, there is a foramen for the caudal (= posterior) middle cerebral vein (Fig. 1.8). The CT scans show that the passage for this blood vessel traverses only the supraoccipital, opening on the most dorsal section of the endocranial cavity (Figs. 7.4, S4). The supraoccipital largely roofs the posterior and posterodorsal regions of the endocranial cavity.

Exoccipital-Opisthotic complex. There are no visible sutures between the exoccipital and opisthotic, as in other adult or juvenile dinosaurs (Currie, 1997). The exoccipital forms the lateral margin of the foramen magnum, whereas the opisthotic probably forms most of the paroccipital process, as observed in a juvenile specimen of the non-sauropodan sauropodomorph *Adeopapposaurus* (PVSJ 610; Martínez, 2009; Paulina-Carabajal, 2009, 2015) (Fig. 1.8).

The exoccipitals form the laterodorsal margins of the rhomboid-shaped foramen magnum, restricting the participation of the supraoccipital at the dorsal margin (Fig. 1.8). Dorsolateral to the foramen magnum, each exoccipital forms a small rounded protuberance that marks the contact with the proatlas, as described for *Piatnitzkysaurus* (Rauhut, 2004). Lateral to the occipital condyle, there are three cranial foramina (Fig. 2.3). The smaller two foramina (4 mm and 2 mm in diameter respectively) are entirely enclosed by the exoccipital and correspond to Cranial Nerve (**CN**) XII (= hypoglossal nerve). The largest foramen (6 mm x 3 mm) is probably enclosed between the exoccipital and the opisthotic (the sutures are not visible in this region) and corresponds to the metotic foramen, for the exit of CNs IX–XI (= glossopharyngeal, vagus, and spinal accessory nerves respectively) and the internal jugular vein (Gower and Weber, 1998). CT scans show a smaller passage—probably the tympanic branch of CN IX—that is anteriorly separate from the larger metotic passage, and exits the braincase through a small foramen located near the columellar recess (Fig. 2.4). The internal foramen of this passage may correspond to the fenestra pseudorotunda. This connection between the metotic passage and the columellar recess (middle ear region) is observed in extant crocodiles (Iordansky, 1973; Witmer *et al.*, 2008; pers. obs. in *Caiman yacare*) and birds (Baumel and Witmer, 1993). When the metotic foramen is subdivided, CNs IX–XI have independent openings, and the terminology of those foramina may be controversial (*e.g.*, Sampson and Witmer, 2007). Gower and Weber (1998) discuss this issue and define that when the metotic fissure of the chondrocranium persists as a single opening it is referred to as the metotic foramen, but when the foramen is subdivided the posterior foramen is named fenestra pseudorotunda (= foramen cochlea, recessus scalae tympani) whereas the anterior foramen corresponds to the jugular foramen (for CN X and the internal jugular vein) (Gow, 1990). Because there is a single internal opening for CNs IX–XI in *Murusraptor*, and a single external opening on the basicranium, the term metotic foramen is used along the text. Externally, the visibility of the metotic foramen only in posterior view of the braincase is a consequence of the development of the *crista tuberalis* (for a

definition of *crista tuberalis* and *crista interfenetralis* in extant reptiles see Säve-Söderbergh, 1947) to such a degree that it separates the lateral and posterior sides of the braincase. In non-sauropodan sauropodomorphs, sauropods, some ornithischians, and some theropods, the *crista tuberalis* is not well developed (the ventral ramus of the opisthotic does not reach the level of the basal tubera); therefore, the most posterior cranial nerves, such as the metotic foramen and CN XII foramina, can be observed in lateral view of the braincase (*e.g.*, Paulina-Carabajal, 2015: fig. 10, and references therein).

The anterior side of the paroccipital process is smooth and its base is slightly convex at the opisthotic-prootic contact (Fig. 1.3). There is no caudal (= posterior) tympanic recess, as in most non-coelurosaur theropods except *Sinraptor* (Paulina-Carabajal and Currie, 2012), and the CT scans confirm that the paroccipital process is an internally solid structure. The opisthotic and the prootic delimit the posterior and anterior margins of the columellar recess, respectively. Posteroventral to the posterior margin of the columellar recess there is a small oval foramen, which corresponds to a passage that splits from the metotic passage, as previously mentioned, probably for the tympanic branch of the glossopharyngeal nerve (*e.g.*, Leblanc, 1992; Witmer *et al.*, 2008) (Fig. 8). The opisthotic-basioccipital suture is barely visible, whereas the contact between exoccipital and basioccipital can be followed on the surface of the occipital condyle and lateral to the basal tuber.

Basioccipital. The basioccipital forms approximately two-thirds of the occipital condyle, the neck of the condyle and posterior section of the basicranium (basal tubera), with a small contribution to the ventral margin of the foramen magnum. It has clear sutures with the exoccipitals and basisphenoid. The basioccipital is the main component of the basal tubera. Both basal tubera are transversely joined by the basituberal web except for their distal ends, which are free. The basituberal web is triangular and posteriorly convex, where it forms a shallow subcondylar pocket ventral to the occipital condyle. The dorsal surface of the neck of the occipital condyle is flat and bears a deep median longitudinal groove (Fig. 1.2, 1.8), also observed in *Piatnitzkysaurus* (PVL 4073) and *Sinraptor* (IVPP 10600). In extant birds, a similar groove is referred to as the *incisura mediana condili*, and represents the impression left by the odontoid process of the axis on the occipital condyle (Baumel and Witmer, 1993). In *Piatnitzkysaurus*, however, the groove has been interpreted as the impression left by the basilar artery (Rauhut, 2004).

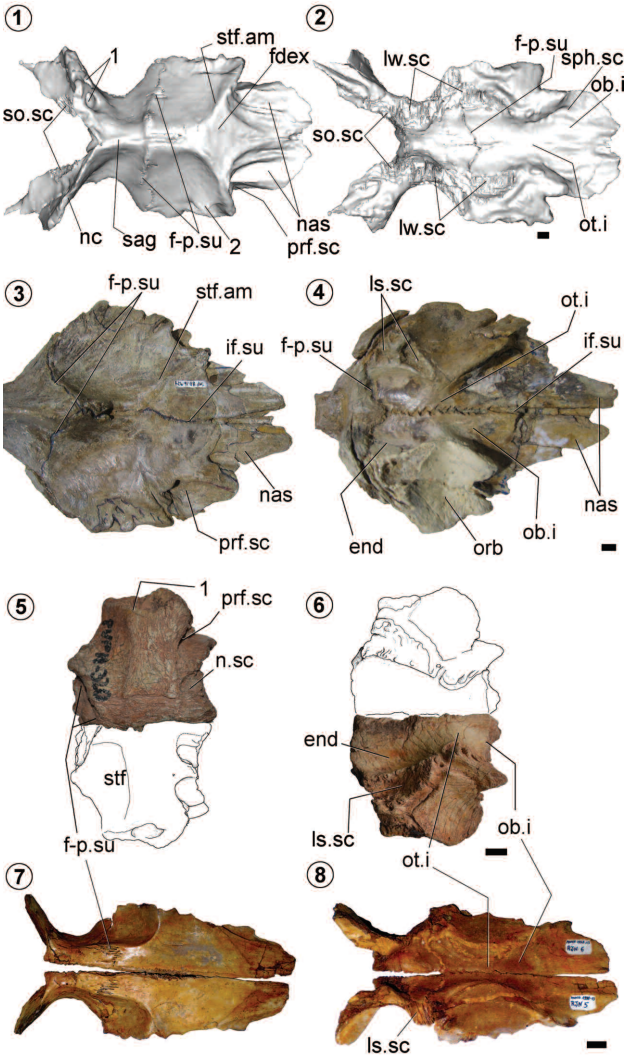

Figure 5. 1–8, Theropod skull roof comparison in dorsal view (left column) and ventral view (right column). **1–2,** 3D virtual reconstruction of the isolated skull roof of ***Murusraptor*** (**MCF-PVPH** 411); **3–4,** indeterminate tyranosaurid **TMP** 80.16.924; **5–6,** left frontal of the theropod **MCF-PVPH** 320 (right frontal reconstructed as line-drawings); **7–8,** ***Dubreuillosaurus*****, MNHN** 1998.13. Abbreviations: **end,** endocranial cavity; **fdex,** exposed dorsal surface of the frontals; **f-p.su,** frontoparietal suture; **if.su,** interfrontal suture; **ls.sc,** surface of contact with laterosphenoid; **lw.sc,** surface of contact with lateral wall of the braincase (opisthotic, prootic, laterosphenoid and orbitoshenoid); **nc,** nuchal crest; **nas,** nasal process of frontal; **n.sc,** surface of contact with nasal bone; **ob.i,** olfactory bulb impression; **orb,** orbital vault; **ot.i,** olfactory tract impression; **prf.sc,** surface of contact with the prefrontal bone; **sag,** sagittal bar; **so.sc,** surface of contact with the supraoccipital bone; **sph.sc,** surface of contact with sphenethmoid; **stf,** supratemporal fossa; **stf.am,** anterior margin of supratemporal fossa; **1,** probable tooth mark?; **2,** pit and triangular shelter, dorsal to the postorbital process of frontal. Scale bars= 10 mm.

Basisphenoid-parasphenoid complex. The basisphenoid contacts the basioccipital posteriorly through visible sutures, the exoccipital-opisthotic complex posterodorsally, and the prootic and laterosphenoid dorsally. However, it is completely fused to the parasphenoid (which forms the cultriform process) anteriorly (Figs. 1.3–4, S5). On the lateral side of the braincase, the basisphenoid-prootic suture is clear and extends horizontally from the *crista tuberalis* to the preotic pendant (Figs. 1.3, 8). The preotic pendant (= *ala basisphenoidalis*) indicates the limit between these two bones in most theropods, but is often formed by both elements to some degree (*e.g.*, Rauhut, 2003; Paulina-Carabajal, 2009, 2015). The mixed composition of the preotic pendant is clearly observed in *Sinraptor* (IVPP 10600) and some tyrannosaurids (*e.g.*, *Daspletosaurus*, TMP 2001.36.01). This projection in generally wing-shaped, and is for the attachment of the *m. protractor pterygoideus* (Holliday, 2009). In *Murusraptor*, the preotic pendant is markedly small when compared to the well-developed alar structure observed in other theropods, such as abelisaurids (*e.g.*, Sampson and Witmer, 2007: fig. 14A; Paulina-Carabajal, 2011b: fig. 4) and tyrannosaurids (*e.g.*, Holliday, 2009: fig. 2K). In *Murusraptor*, the basisphenoid-laterosphenoid suture is barely visible and the contact is anterodorsal to the preotic pendant. Posterolaterally, the basisphenoid contacts the ventral branch of the opisthotic at the distal end of the *crista tuberalis* along a vertical suture.

The basicranium is the region of the braincase most affected by pneumaticity, where basisphenoidal, lateral tympanic and basipterygoid recesses can be identified (Fig. 4). The basituberal web (formed by the basioccipital in *Murusraptor*) forms the posterior wall of the basisphenoidal recess, which is deeply excavated on the ventral side of the basisphenoid and delimited between the basal tubera and the basipterygoid processes (Fig. 1.6). The lateral walls of the basisphenoid recess are formed by thin laminae of the basisphenoid bone (= *crista ventrolateralis*), which join the basal tuber with the basipterygoid process of each side. The ventral margin of the *crista ventrolateralis* expands posterolaterally, enlarging the volume of the basisphenoidal recess, as in *Allosaurus* (USNM 544100, UUVP 5961). In *Murusraptor*, the basisphenoid recess is ventrally oriented, and therefore is not observed in a posterior view of the braincase. Inside the cavity, which narrows dorsally, there are two oval pneumatic openings separated by a thin median septum. The CT scans reveal that these openings communicate with pneumatic cavities within the basisphenoid and basioccipital. On the lateral side of the basisphenoid, the preotic pendant partially overhangs the reduced opening of the lateral (= rostral) tympanic recess (Figs. 1.4, 2.1). The CT scans revealed the internal extent of this recess, which is larger than the external opening. The internal carotid artery enters the braincase through the ventral section of the lateral tympanic recess on its way into the pituitary fossa (Figs. 1.4, 2.4). The third pneumatic recess corresponds to the basipterygoid recess, a small and oval opening on the lateral side of each basipterygoid process (Fig. 1.4).

Endocranially the basisphenoid forms most of the floor of the endocranial cavity, from the foramen magnum threshold to the *dorsum sellae* (Fig. 4). The floor of the endocranial cavity is narrow and mostly flat (Fig. S5.9). The two small internal foramina for CN VI (= abducens nerve) open just posterior to the dorsum sellae, and near to the midline. The passages for CNs VI are anteroventrolaterally oriented, extending lateral to the pituitary fossa and exiting the braincase through small and circular external foramina (Figs. 2.2, S5.8). The *dorsum sellae* is not strongly projected dorsally, as in most theropods. The infundibulum (hosting the infundibular stalk) is an oval opening connecting the endocranial cavity with the pituitary fossa ventrally. The rounded pituitary fossa projects ventrally and excavates the basisphenoid. The lateral walls of the pituitary fossa are delicate and extremely thin laminae, pierced by a small blood vessel foramen on each side, probably for the sphenoid artery (Baumel and Witmer, 1993; Witmer and Ridgely, 2008; Miyashita *et al.*, 2011). The posterior wall of the pituitary fossa is pierced by two separate foramina for the entrances of the left and right cerebral internal carotid arteries.

The cultriform process, formed probably only by the parasphenoid, is a delicate and short, rod-shaped structure, unlike the blade-shaped and elongate cultriform processes observed in other non-coelurosaur theropods such as *Allosaurus* (UUVP 5961), *Piveteausaurus* (MNHN 1920-7), *Sinraptor* (Currie and Zhao, 1993a; Paulina-Carabajal and Currie, 2012), or abelisaurids (*e.g.*, Sampson and Witmer, 2007; Paulina-Carabajal, 2011b; Filippi *et al.*, 2016). In *Murusraptor*, the base of the process is laterally compressed and solid, and it is excavated dorsally by a longitudinal

groove, although its base is smooth. There is no subsellar recess (Fig. 1.6).

Prootic. In *Murusraptor* the prootic contacts the basisphenoid, laterosphenoid, opisthotic, and parietal through clear sutures observed externally on the braincase. The prootic-opisthotic contact is particularly clear (Figs. 1.4, 2.4). The posterior wing of the prootic overlays the opisthotic, where it overhangs the columellar recess ventrally. The latter is a triangular opening, enclosed between the prootic and the opisthotic. The prootic forms the posterior margin of the large CN $V_{2,3}$ (= maxillomandibular trigeminal branch) foramen (Figs. 2.4, S4.3). The opening for CN V_1 (= ophthalmic branch of the trigeminal nerve) is separate and exits the braincase through a small foramen enclosed by the laterosphenoid. The foramen for CN VII (= facial nerve) is enclosed by the prootic, and is located posterior to the foramen for CN $V_{2,3}$. It is a small and narrow, hourglass shaped opening generated by a constriction that separates the palatine and the hyomandibular branches of the facial nerve. Those branches leave shallow impressions as grooves extending posteriorly and ventrally respectively from the CN VII foramen (Fig. 2.4).

Endocranially the prootic probably forms a large section of the vestibular eminence, as interpreted from the location of the cranial nerve foramina. On the dorsal surface of the vestibular eminence, there is a vertical suture between the prootic and another bone that may correspond to the epiotic (which is fused in turn to the supraoccipital). A similar suture is also observed on the vestibular eminence of the abelisaurid *Aucasaurus* (Paulina-Carabajal, 2011a: fig, 9A). The floccular recess of *Murusraptor*, excavated on the anterior side of the vestibular eminence, is a relatively small oval cavity, as in most non-avian theropods (*e.g.*, Rauhut, 2004; Sampson and Witmer, 2007; Witmer and Ridgely, 2009; Paulina-Carabajal and Currie, 2012) except maniraptorans (*e.g.*, Currie and Zhao, 1993b; Lautenschlager *et al.*, 2012; Fig. S4.6). The foramen or foramina for CN VIII (= vestibulocochlear nerve) was/were probably very small, and therefore is/are not observed in the CT scans.

Laterosphenoid. As in other dinosaurs, the laterosphenoid forms a large section of the lateral wall of the braincase. The postorbital process of the laterosphenoid of *Murusraptor* is finger-shaped and projects dorsolaterally. It has a deep circular pit anteroventrally that corresponds to the impression left by the contact with the epipterygoid (Fig. S6.5). A well-defined contact is not observed in other studied theropods, which in general have only small shallow depressions, as observed in *Carnotaurus* (MACN-CH 894), *Sinosaurus* (Xing *et al.*, 2014), *Troodon* (TMP 82.19.23), and *Tyrannosaurus* (LACM 150167). In some theropods, the contact may not be evident at all as in *Giganotosaurus* (MUCPV-CH-1) and *Sinraptor* (IVPP 10600).

In *Murusraptor*, the laterosphenoid-orbitosphenoid suture is obscured by fusion, and the limit between both elements is defined by the location of the foramina for CN III (= oculomotor nerve) and CN IV (= trochlear nerve), which are enclosed between both elements in most theropods (Currie, 1997). In *Murusraptor*, CN III and CN IV are respectively ventral and anterior to the postorbital process of the laterosphenoid (Fig. 1.4, 1.6). The foramen for CN III is circular and 4 mm in diameter, and is positioned posterior to that for CN II (= optic nerve). The foramen for CN IV is smaller, slit-like, and anterodorsal to the opening for CN III. The orbitocerebral vein apparently exited the endocranial cavity together with CN IV (Fig. 2.2). The openings for CN III and IV are oriented anteriorly and can not be observed in the lateral view of the braincase.

The parietal-laterosphenoid suture forms an inverted V, and is somewhat sinuous posteriorly; in contrast, the frontal-laterosphenoid suture is anteroposteriorly short. As mentioned, the laterosphenoid forms the anterior margin of the foramen for CN $V_{2,3}$ and encloses the foramen for CN V_1. Separate openings for the ophthalmic branch are also observed in other theropods, such as abelisaurids (Sampson and Witmer, 2007; Paulina-Carabajal, 2011a, b). This contrasts with the single foramen present in *Giganotosaurus* (MUCPV-CH-1), or the incipient separated branch observed in *Sinraptor* (Currie and Zhao, 1993a). A shallow and subhorizontal crest—developed dorsal to CN V_1 and ventral to the postorbital process of the laterosphenoid—may indicate the osteological correlate for *m. levator pterydoideus* (Holliday, 2009).

Orbitosphenoid. The orbitosphenoid contacts the frontal dorsally through a partially open suture and the laterosphenoid posteriorly through a suture obscured by fusion. The orbitosphenoid probably contacts the basisphenoid for a short distance ventrally, and contacts its counterpart anteroventrally, delimiting the lateral and ventral margins of

the large opening for the olfactory tracts (indicated as CN I in Figure 2.2). Both foramina for CN II are confluent anteroventrally on the midline, forming an elongate opening, which is wider than high. The inter-orbitosphenoid suture is vertical, and is clearly observed dorsal to CN II.

Ethmoidal complex. In *Murusraptor*, the ethmoidal elements (sphenethmoids + mesethmoid; Ali *et al.*, 2008) are ossified and disarticulated from the braincase. The sphenethmoids form a U-shaped element that ventrolaterally encloses the cavities occupied by the olfactory tracts and bulbs (Fig. 3). Anteroventrally, the sphenethmoid bears a median septum—probably formed by the mesethmoid—that separates the cavities occupied by left and right olfactory bulbs. The sphenethmoids dorsally contact the frontals, fitting into two parasagittal slits excavated into the ventral surfaces of the frontals (Fig. 5.2). When in position, there is an unossified space between the orbitosphenoid and the sphenethmoid. The space is 20 mm long on the midline and 9 mm laterally, and corresponds to an unossified posterior section of the sphenethmoid or to an unossified septosphenoid (*e.g.*, Paulina-Carabajal and Currie, 2012). U-shaped sphenethmoids are present in *Murusraptor* and *Sinraptor* (Paulina-Carabajal and Currie, 2012). Other theropods with preserved ethmoidal elements, such as the megalosaur *Piveteausaurus* (MNHN 1920-7), carcharodontosaurids (MUCPV-CH-1, SGM-Din 1; Franzosa and Rowe, 2005), neoceratosaurs (Sanders and Smith, 2005; Sampson and Witmer, 2007; Paulina-Carabajal, 2011a, b), and tyrannosaurids (*e.g.*, Brochu, 2003; Ali *et al.*, 2008) have tube-like sphenethmoids that exclude the frontals from the roof of the olfactory bulb cavities. In the case of the subadult tyrannosaurid *Daspletosaurus* (TMP 2001.36.01), the right and left sphenethmoids are not connected dorsally at the midline, suggesting that the dorsal closure forms late during ontogeny.

Braincase pneumaticity

There are well recognized pneumatic cavities in the braincases of theropod dinosaurs, derived from extensions of the nasal cavity, the tympanic cavity, and the median pharyngeal system. Similarly, some of the pneumatic cavities found in certain theropod dinosaurs (*e.g.*, subcondylar recess) may result from pulmonary diverticula (Witmer, 1997; Witmer *et al.*, 2008; Dufeau, 2011). In *Murusraptor*, the CT scans revealed the extent of the lateral (= rostral) tympanic recess, the basisphenoidal recess, and the basipterygoid recesses (Figs. 6, S7–S9). All these pneumatic recesses are found in the basicranium, developed particularly within the basisphenoid.

The lateral (= anterior) tympanic recess is derived from pneumatic diverticula of the middle ear sac (Witmer, 1997; Witmer and Ridgely, 2009; = "pharyngotympanic sinus" in Dufeau, 2011), whereas the basisphenoidal recess probably develops from a diverticulum of the pharynx separated from the middle ear sac (Witmer and Ridgely, 2009; = "median pharyngeal sinus" in Dufeau, 2011). The pneumatic origin of the basipterygoid recess is less certain (Witmer, 1997). Dufeau (2011) believes it is an anterior expansion of the pharyngotympanic sinus (which also forms the lateral tympanic recess). This seems to be true in *Murusraptor* where both external openings for the lateral tympanic and basipterygoid recesses are within the same large but shallow depression on the lateral side of the basicranium. The posterodorsal margin of this depression is anteriorly concave, and clearly observed in lateral view. In non-coelurosaur theropods, the basicranium is the most pneumatic region of the braincase (Paulina-Carabajal, 2008, 2015). Therefore, the braincase of *Murusraptor* has poorly developed pneumatic recesses compared with those of coelurosaurs, such as tyrannosaurids (*e.g.*, Witmer and Ridgely, 2008, 2009; Dufeau, 2011), in which the caudal tympanic recesses are well-developed, affecting the paroccipital processes and the supraoccipital.

In *Murusraptor*, the external opening of the lateral tympanic recess is a small and triangular opening on the lateral side of the basisphenoid. Anterodorsally, the small preotic pendant overhangs this opening. The internal carotid artery enters the basicranium through this opening. A reduced external opening for the lateral tympanic recess is also present in *Sinraptor* (Currie and Zhao, 1993a; Paulina-Carabajal and Currie, 2012), and tyrannosaurids (*e.g.*, Currie, 2003). In *Dromaeosaurus*, there is no development of the lateral tympanic recess and the internal carotid artery has a small foramen clearly visible in lateral view (Currie, 1995: fig. 6). In other theropods, such as abelisaurids (*e.g.*, Sampson and Witmer, 2007; Paulina-Carabajal, 2011a, b), the megalosaur *Piatnitzkysaurus* (Rauhut, 2004; Paulina-Carabajal, 2009), the spinosaurids *Baryonyx* (Charig and Milner, 1997; BMNH R9951) and *Irritator* (Sues *et al.*, 2002;

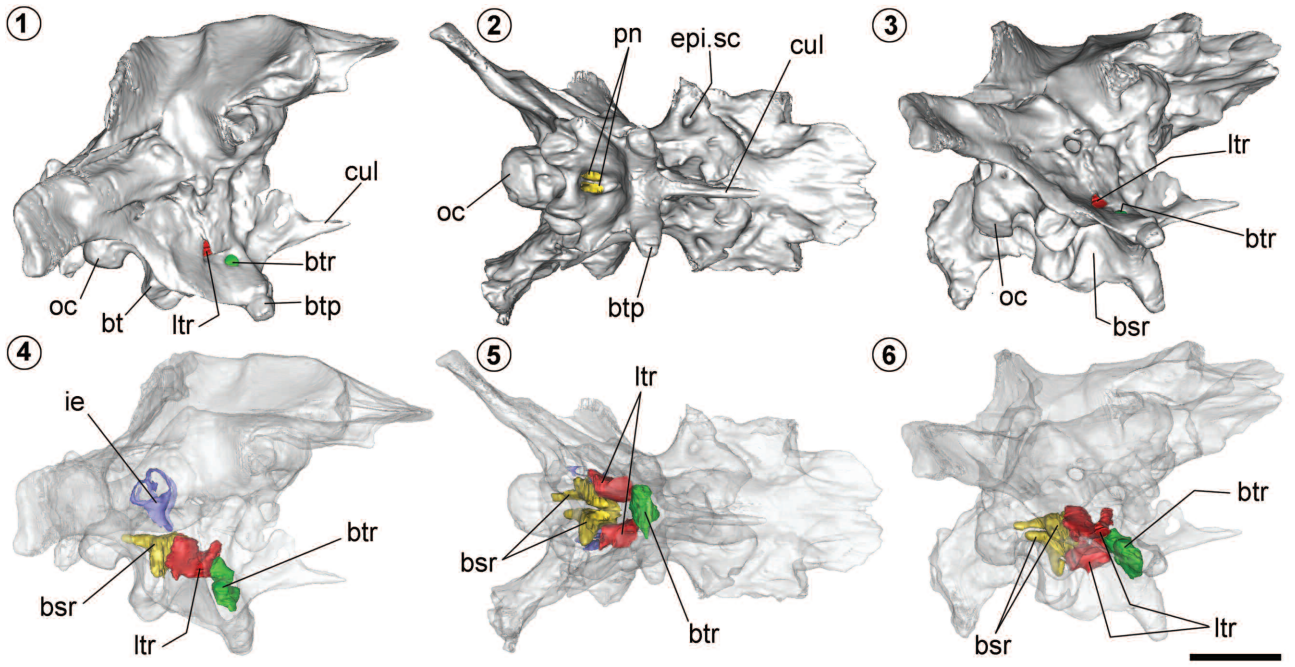

Figure 6. 1–6, Braincase pneumaticity of ***Murusraptor*** **(MCF-PVPH** 411). Volume-rendered CT-based reconstruction of the braincase and pneumatic cavities. **1, 4,** lateral view; **2, 5,** ventral view; **3, 6,** lateroventral view. The bone in Figures **4–6** is rendered semitransparent to allow observation of the internal cavities: basisphenoid recess (yellow), lateral tympanic recess (red) and basipterygoid recess (green). Abbreviations: **bsr,** basisphenoidal recess; **bt,** basal tuber; **btr,** basipterygoid recess; **btp,** basipterygoid process; **cul,** cultriform; **epi.sc,** surface of contact with epipterygoid; **ie,** inner ear; **ltr,** lateral tympanic recess; **oc,** occipital condyle; **pn,** pneumatic foramina. Scale bar= 50mm.

SMNS 58022), and *Troodon* (TMP 82.19.23; Currie and Zhao, 1993b), the lateral tympanic recesses are well developed (*e.g.*, Paulina-Carabajal, 2015 and references therein). The size of the external opening of the lateral tympanic recess does not necessarily reflect the internal extent of the pneumatic recess. In *Murusraptor*, the right and left lateral tympanic recesses excavate the basisphenoid internally without contacting each other medially (Fig. 6.5). Each lateral tympanic recess develops two main lobes—a smaller one anteriorly and a markedly larger lobe posteriorly—separated by a strong vertical constriction (Fig. S7). The anterior lobe is a tubular expansion that continues distally into the passage of the internal carotid artery. The posterior lobe extends posterodorsally to reach the level of the dorsal section of the basisphenoid recess (Fig. 6.4).

In *Murusraptor*, the basisphenoid recess is deeply excavated on the ventral side of the basisphenoid (Figs. 1.6, S8). Within the deepest part of the basisphenoidal recess there are two elongate foramina. The CT scans show that these foramina extend posteriorly as finger-like projections that enter the neck of the occipital condyle (Fig. 6.4). In coronal slices of the CT scans, these projections are observed as two parasagittal canals, approximately 4.2 mm in diameter that extend parallel within the neck of the condyle without reaching the occipital condyle. The right canal is longer than the left one, which is affected by the paleopathology. Similar cavities are known in abelisauroids, such as *Aucasaurus* (MCF-PVPH 236), *Ilokelesia* (MCF-PVPH 35), *Ekrixinatosaurus* (MUCPV 294) (Paulina-Carabajal, 2011a: fig. 4), and *Viavenator* (MAU-Pv-LI-530; Filippi *et al.*, 2016), and in the carcharodontosaurids *Carcharodontosaurus* (Coria and Currie, 2002a) and *Giganotosaurus* (MUCPV-CH-1).

The oval basipterygoid recess opens on the lateral side of the basipterygoid process. The CT scans show that the basipterygoid recess communicates internally with a larger pneumatic cavity at the base of the process (Fig. 6.4). This is an irregular cavity, separated from its counterpart by a thin median longitudinal septum. In coronal view, this septum is incomplete dorsally, and there is a small connection between the right and left pneumatic cavities (Fig. S9).

Cranial endocast

The complete cranial endocast of *Murusraptor*, measured from the olfactory bulb to the foramen magnum, is approximately 116 mm in total anteroposterior length (Fig. 7). The forebrain and hindbrain are sub-horizontal, with the midbrain angled between them. The forebrain-midbrain and midbrain-hindbrain angles (approximately 125° and 55° respectively) are similar to those observed in other non-maniraptoran theropods (*e.g.*, Witmer and Ridgely, 2009). *Murusraptor* has a relatively short midbrain and CN V is aligned vertically to the dorsal expansion (= dural peak) (Fig. 7.4), which is similar to the condition observed in *Tyrannosaurus* (Witmer and Ridgely, 2009: fig. 1A). The midbrain is relatively more elongate in carcharodontosaurids (Larsson, 2001; Paulina-Carabajal and Canale, 2010) and ceratosaurs (*e.g.*, Sanders and Smith, 2005; Sampson and Witmer, 2007; Paulina-Carabajal and Succar, 2015; Paulina-Carabajal and Filippi, 2016), in which the dural expansion is relatively more anterior in relation to CN V. The shortening of the midbrain maybe related to the stronger angling of the brain in the coelurosaurs (Rauhut, pers. comm. 2016); however, in allosauroids and ceratosaurs the length of the medulla (measured from the foramen magnum to CN V) is shorter than the midbrain section (measured from the anterior border of the flocculus to the dorsal expansion).

As in other non-maniraptoran theropods, there are no vascular impressions on the cranial endocast, which indicates that the dorsal longitudinal venous sinus and the dura mater are large enough to obscure the morphology of the encephalic structures (Hopson, 1979; Franzosa, 2004; Evans, 2005; Witmer *et al.*, 2008). In addition, the endocast of *Murusraptor* shows the positions of the open sutures between the frontals and parietals, and between the skull roof and the lateral walls of the braincase (Figs. 7.2, 7.4, S1). The dorsal expansion represents the extent of the dorsal longitudinal venous sinus (Witmer *et al.*, 2008; Knoll *et al.*, 2012 and discussion therein) and projects slightly dorsally above the level of the forebrain in lateral view.

Forebrain. The outstanding features of the forebrain of *Murusraptor* include the olfactory tracts and olfactory bulbs (indicated as CN I in Figure 7.2), the cerebral hemispheres, optic nerves (CN II), the infundibular stalk, and the pituitary body. The shape and size of the olfactory bulbs is known based on the impression left on the ventral side of the frontals, and from a latex endocast of the cavities enclosed by the sphenethmoids (Figs. 3, 7.1).

The olfactory tract and bulbs are aligned horizontally with the rest of the forebrain. The olfactory tract of *Murusraptor* is 20 mm wide and 20 mm long. It is relatively short when compared with the enlarged tracts of carcharodontosaurids (Larsson, 2001; Paulina-Carabajal and Canale, 2010) and ceratosaurs (Sampson and Witmer, 2007; Paulina-Carabajal and Succar, 2015; Paulina-Carabajal and Filippi, 2016), which have elongate and robust olfactory tracts and elongate olfactory bulbs (in the mentioned taxa, the lengths of the olfactory tracts and bulbs equal the lengths of the rest of the entire endocast). The olfactory tracts are robust and short in other theropods, such as the possible megaraptorid MCF-PVPH 320 (Paulina-Carabajal and Coria, 2015) (Fig. 5.6) and tyrannosaurids (Fig. 5.4). The olfactory bulbs of *Murusraptor* are large, elongate and oval in dorsal view, and slightly divergent anteriorly (Fig. 7.2).

The dorsal morphology of the cerebral hemispheres is obscured by the sagittal longitudinal sinus. The maximum transverse width of the endocast is 40 mm, measured at the level of the cerebral hemispheres, which are not markedly expanded laterally.

The passages of the CNs II are short and broad. They are confluent and exit the braincase through a large, single, hourglass-shaped opening, are oriented anteriorly, and can be seen clearly in the endocast. The optic tract and the base of the infundibulum converge in a rounded area ventral to the cerebral hemispheres that probably represents the cast of the recess enclosing the optic chiasm. Although the optic lobes are not well developed, the presence of large passages for the optic nerves and the probable presence of enlarged optic tracts suggest some degree of dependence on visual capabilities for this taxon.

The infundibular stalk is short, and oriented vertically. Immediately beneath it, the oval, laterally compressed pituitary body descends from the ventral surface of the endocast. A small blood vessel can be seen on each side of the pituitary gland. Similar blood vessels have been identified by other authors as the "pituitary vein", "ophthalmic artery", and "palatine artery", in ankylosaurs (Tumanova, 1987; Norman and Faiers, 1996) or the "sphenoid artery" in sauropods (Sues *et al.*, 2015; "pituitary vein" in Paulina-Carabajal, 2012), the ceratopsid *Pachyrhinosaurus* (Witmer and Ridgely,

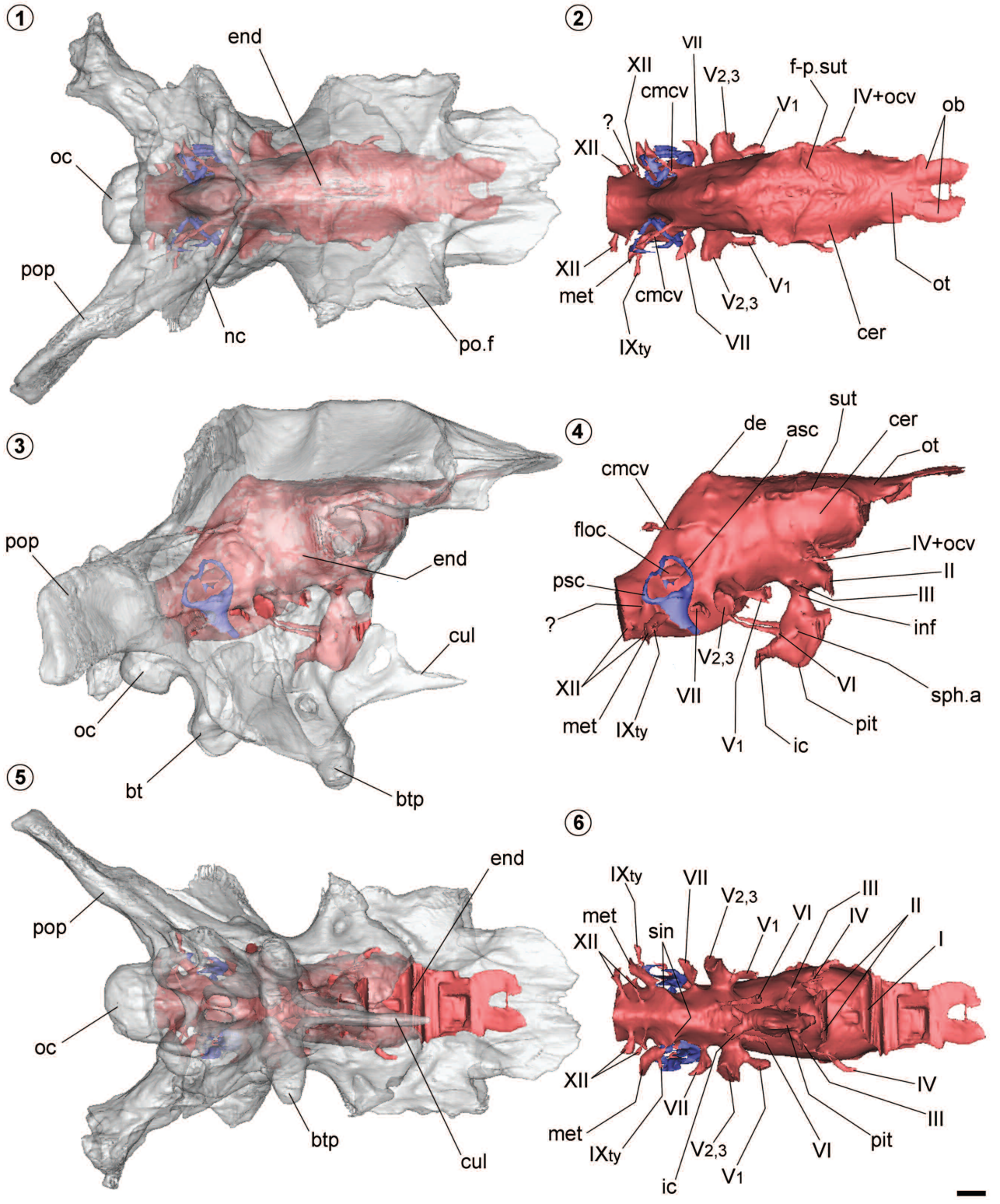

Figure 7. Volume-rendered CT-based reconstruction of the braincase (left column) and cranial endocast (right column) of ***Murusraptor*** **(MCF-PVPH** 411). The bone is rendered semitransparent to show the endocranial cavity. **1–2,** dorsal view; **3–4,** right lateral view; **5–6,** ventral view. Abbreviations: **asc,** anterior semicircular canal; **bt,** basal tuber; **btp,** basipterygoid process; **cer,** cerebral hemisphere; **cmcv,** caudal middle cerebral vein; **cul,** cultriform process; **end,** endocranial cast; **de,** dorsal expansion; **floc,** flocculus of cerebellum; **f-p.sut,** cast of the frontoparietal suture; **ic,** internal carotid artery; **inf,** infundibulum; **met,** metotic passage for CNs IX–XI; **nc,** nuchal crest; **ob,** olfactory bulb; **oc,** occipital condyle; **ocv,** orbitocerebral vein; **ot,** olfactory tract; **pit,** pituitary; **po.f,** postorbital process of frontal; **pop,** paroccipital process; **psc,** posterior semicircular canal; **sin,** venous sinus; **sph.a,** sphenoid artery entering the pituitary fossa; **sut,** cast of suture; **I–XII,** cranial nerves; **IX_{ty},** tympanic branch; **?,** endolymphatic duct?. Scale bar= 10 mm.

2008), and the abelisaurid theropod *Majungasaurus* (Sampson and Witmer, 2007). The terminology used by Sampson and Witmer (2007), who interpret these vascular passages in dinosaurs as the sphenoidal artery as in extant birds (Baumel and Witmer, 1993), is used in this paper.

Midbrain. The only visible mesencephalic structures of *Murusraptor* are the passages of CNs III and IV. The optic lobes are not clearly defined, as in the other studied non-maniraptoran theropods (Franzosa, 2004). A peculiarity of the midbrain region of *Murusraptor* is that it is relatively short, so that the midbrain is similar in length to the medulla oblongata. As mentioned, this is also observed in the cranial endocast of *Tyrannosaurus* (*e.g.*, Hopson, 1979; Witmer and Ridgely, 2009). Non-coelurosaur Tetanurae and Ceratosauria have markedly elongate midbrains (the length of this section of the cranial endocast, measured from the flocculus to the dorsal expansion, surpasses the length of the medulla).

In *Murusraptor*, CN III is circular and is located posterior to CN II and ventral to CN IV (Fig. 8.2). The root of the passage for CN III is positioned on the most posterior section of the expansion identified as a probable "optic chiasm", and the passage extends slightly forwards. Cranial nerve IV has a smaller passage in diameter, is anterodorsal to CN III, and is widely separated from it. The passage expands distally into a slit-like external foramen. The orbitocerebral vein exits dorsally the endocranial cavity through the same foramen.

Hindbrain. The visible features in the hindbrain of the cranial endocast include the cerebellum, medulla oblongata, and CNs V–XII. The cerebellum is not clearly expanded in the endocast. However, the floccular process of the cerebellum is well defined (Fig. 7.4). The flocculus of the cerebellum is a relatively small process in most dinosaurs (when compared to those of flying reptiles and avian theropods; see Witmer *et al.*, 2003 and references therein). In *Murusraptor*, the slightly flattened and relatively elongate flocculus projects posterolaterally, extending far beyond the anterior semicircular canal to almost reach the posterior semicircular canal. Similarly flattened and elongate flocculi are present in abelisaurids (Sampson and Witmer, 2007; Paulina-Carabajal and Succar, 2015). In non-coelurosaurian theropods (*Acrocanthosaurus*, *Allosaurus*, *Ceratosaurus*) and adult *Tyrannosaurus* specimens (Witmer and Ridgely, 2009), the flocculus generally has a tabular shape, whereas in other coelurosaurs it tends to be relatively larger with a rounded base, and often a distal swelling (*e.g.*, *Dromaeosaurus*, *Struthiomimus*, *Troodon*; Witmer and Ridgely, 2009).

The ventral surface of the medulla oblongata is narrow and nearly flat posteriorly but becomes convex anteriorly, where the ridges extending from the metotic passages (impressions of large blood vessels or sinuses) join the base of the medulla. This indicates the presence of a longitudinal ventral blood sinus along the floor of the endocranial cavity, probably the basilar artery, as identified by Rauhut (2004) in *Piatnitzkysaurus*. Laterally, on each side of the medulla oblongata, and dorsal to CN XII, there is a small lateral projection, enclosed in a poorly preserved canal or pit (Figs. 7.4, 8.2). CT scans do not show the path of this passage, suggesting it is the cast of a blind canal or that it has such a small diameter that is not observed in the CT scans. Kurzanov (1976: fig. 3A) illustrates the same structure in the medullar cavity of *Itemirus*, and identified it as an endolymphatic duct. Alternatively, this could be a small diverticulum of the longitudinal sinus (S. Lautenschlager, pers. comm).

Internally, all the branches of the trigeminal nerve (CN V) leave the endocranial cavity through a single foramen. In the endocast, the root (stem) of the trigeminal nerve is a large passage that extends transversally. The ophthalmic branch (CN V_1), which has a smaller diameter, separates in an angle of 90° from the maxillomandibular branches and projects anterolaterally. The bifurcation of CN V_1 and $V_{2,3}$ corresponds to an enlarged region of the main passage that indicates the location of the trigeminal ganglion (Holliday and Witmer, 2007) (Fig. 8.2). The intracranial position of the trigeminal ganglion is a derived condition found in extant birds (Witmer *et al.*, 2008). A similarly diverging ophthalmic branch of the trigeminal nerve is commonly found among tetanurans (*e.g.*, *Allosaurus*, *Dromaeosaurus*, *Troodon*); tyrannosaurids, however, have ophthalmic and maxillomandibular canals that branch separately from the endocranial cavity (Witmer and Ridgely, 2009).

Cranial nerve VI has a small passage that expands distally. Right and left passages project anteroventrolaterally from the ventral side of the medulla and pass laterally to the pituitary (Fig. 7.4). In *Murusraptor*, the abducens nerves are the longest of the cranial nerves; in ventral view, they

are not markedly divergent from the midline (Fig. 7.6).

The root of the passage of CN VII is just posterior to that of CN V and has a smaller diameter than its distal end, which is enlarged and semilunate (Fig. 8.1). This morphology respectively reflects the dorsal and ventral separation of the hyomandibular and palatine branches of the facial nerve. As mentioned, the hyomandibular branch (and probably the palatine artery; Gower, 2002) leaves a groove on the lateral surface of the prootic, indicating its posteriorly oriented path from the CN VII foramen, whereas the palatine branch leaves a ventrally oriented groove.

It was not possible to identify CN VIII using the CT scans. Considering the excellent preservation of the specimen, this suggests that the foramen or foramina for this nerve on the vestibular eminence is/are markedly small in diameter.

In *Murusraptor*, CNs IX–XI exit the endocranial cavity through a single internal metotic foramen. On the cranial endocast, the root of this large passage is cylindrical and large in diameter, and merges with a vertical venous sinus that extends anteroventrally to form a crest on the lateroventral side of the medulla oblongata (Figs. 7.4, 8.2). The passage is posterolaterally oriented and its distal end corresponds to the external metotic foramen, which opens posterior to the *crista tuberalis*. A smaller passage separates from the main metotic canal and extends anterolaterally to exit through a small foramen anterior to the *crista tuberalis*, near the columellar recess. The close vicinity of this passage to the middle ear region of the braincase indicates that it probably corresponds to the tympanic branch of CN IX. Most non-coelurosaur theropods where this region is known have undivided metotic passages. However, the presence of a separate passage for CN IX (glossopharyngeal nerve) that exits the braincase through an opening anterior to the *crista tuberalis* is not uncommon. This is a feature shared with *Acrocanthosaurus* (Franzosa and Rowe, 2005; these authors mentioned a probable separate exit for the glossopharyngeal nerve observed on the left side of the braincase only), *Allosaurus* (Witmer and Ridgely, 2009; although this can not be seen in the specimen USNM 544100, pers. obs.), and coelurosaurs, such as *Alioramus* (Bever *et al.*, 2011), *Iterimus* (= fenestra rotunda, Kurzanov, 1976), and *Tyrannosaurus rex* (Witmer and Ridgely, 2009: fig. 5A). In tyrannosaurids the glossopharyngeal nerve did not extend through the vagal canal, but rather passed anterior to the *crista tuberalis* through a separate canal (= *recessus scalae tympani*, leading into the foramen pseudorotunda, in Bever *et al.*, 2011) anterior to the vagal canal and ventral to the columellar canal (Witmer and Ridgely, 2009). The condition observed in *Murusraptor* is not exactly the same, and CNs IX–XI share the same root en-

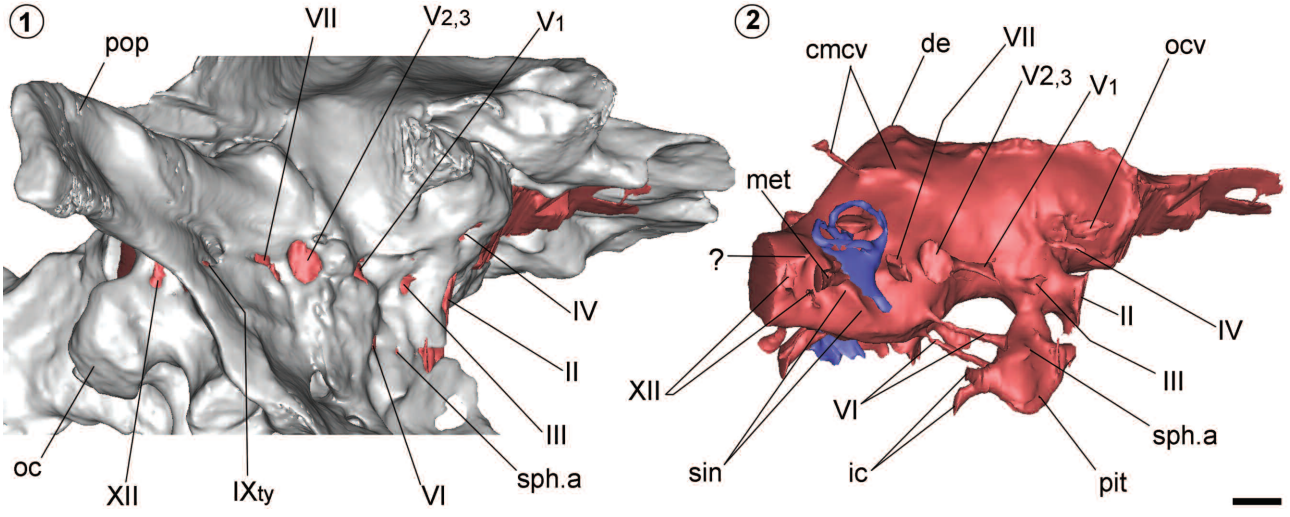

Figure 8. 1, Volume-rendered CT-based reconstruction of the braincase and **2,** cranial endocast of ***Murusraptor*** **(MCF-PVPH** 411) in right lateroventral view. Abbreviations as in Figure 7. Scale bar= 10 mm.

docranially, although CN IX separates before exiting the braincase. A single root and passage for CN IX–XI is also present in other non-coelurosaur theropods such as the allosauroids *Acrocanthosaurus* (Franzosa and Rowe, 2005), *Allosaurus* (Witmer and Ridgely, 2009), *Giganotosaurus* (Paulina-Carabajal and Canale, 2010), and *Sinraptor* (Paulina-Carabajal and Currie, 2012), the ceratosaurs *Ceratosaurus* (Sanders and Smith, 2005), *Majungasaurus* (Sampson and Witmer, 2007), as well as *Sinosaurus* (Xing *et al.*, 2014). It is also present in other theropods, such as therizinosaurs (Lautenschlager *et al.*, 2012). In the mentioned taxa, the metotic passage projects posteriorly and CN IX–XI exit posterior to the *crista tuberalis*.

All the branches for CN XII exit the endocranial cavity through two sub-horizontally aligned foramina (Fig. 8). The posterior passage is the largest and extends slightly posterolaterally from the base of the medulla oblongata. The anterior passage has a smaller diameter, and is slightly closer to the midline than the posterior passage.

Blood vessels. There are only three sets of vascular foramina in the braincase of *Murusraptor*. One corresponds to a vein and the other two to arteries. The caudal middle cerebral vein pierces the supraoccipital and extends anteroventrally to the posterodorsal section of the endocast, where it merges with the dorsal expansion and the dorsal longitudinal venous sinus (see Witmer *et al.*, 2008). The root of this passage is vertically aligned with CN VII. As mentioned previously, there is no foramen for the rostral middle cerebral vein, indicating that this blood vessel exits the braincase together with the trigeminal nerve. On the lateral side of the cranial endocast, a shallow ridge extends from the caudal middle cerebral vein towards the root of CN V, and represents a transverse venous sinus (Witmer and Ridgely, 2009). Furthermore, the ventral longitudinal venous sinus (Sampson and Witmer, 2007) cannot be clearly seen in the endocast except in the most posteroventral region of the medulla oblongata (Fig. 8.2).

The orbitocerebral vein is small and exits the endocranial cavity through a slit-like foramen together with CN IV (Fig. 8.2).

The internal carotid artery enters the braincase through the lateral tympanic recess which is why the distal end of the passage has an irregular shape. The canal for the internal carotid artery is large in diameter and short. It extends anteromedially to join its counterpart before entering the pituitary fossa (Fig. 8.2). A small and markedly short passage for the sphenoidal artery is on each side of the pituitary cast.

Inner ear. The inner ear morphology of *Murusraptor* is partially reconstructed on both sides. The semicircular canals are slender and similar in diameter with the common crus (Fig. 9). The inner ear is 37.3 mm long dorsoventrally and has a maximum width of 22.9 mm at the level of the semicircular canals. The anterior semicircular canal (**ASC**) is larger than the posterior semicircular canal (**PSC**), whereas the lateral semicircular canal (**LSC**) is smaller than the other two. The outlines of the ASC and PSC are oval, but the lateral semicircular canal is a lateromedially compressed ellipse. The ASC is higher than the PSC and rises above the common crus (Fig. 9.1). The angle formed between the ASC and PSC is approximately 80° in dorsal view (Fig. 9.2), whereas the same angle is approximately 45° in *Allosaurus* (Rogers, 1999), and 85° in *Ceratosaurus*. The angle seen in *Ceratosaurus* is close to that seen in most non-coelurosaur theropods (Sanders and Smith, 2005) (Tab. 1).

Although the margins of the oval window are not clear, its position is inferred from the location of the columellar recess. The lagena is approximately 9–11.5 mm long, which is 25–30% the length of the total inner ear.

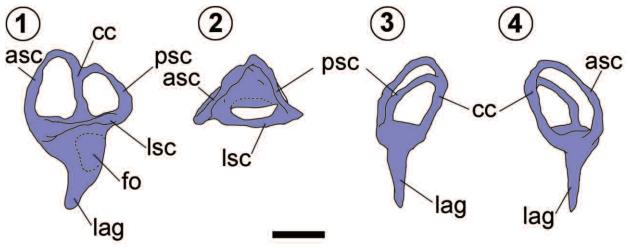

Figure 9. Left inner ear of ***Murusraptor*** (**MCF-PVPH** 411); line-drawing based on the volume-rendered CT-based reconstructions of left and right inner ears; **1,** lateral view; **2,** dorsal view; **3,** posterior view; **4,** anterior view. Abbreviations: **asc,** anterior semicircular canal; **cc,** common crus; **fo,** fenestra ovalis; **lag,** lagena; **lsc,** lateral semicircular canal; **psc,** posterior semicircular canal. Scale bar= 10 mm.

SENSORIAL AND COGNITIVE CAPABILITIES

A general evaluation of the sensory and cognitive capabilities of theropods can be made based on certain

measurements of the reconstructed endocranial features (Lautenschlager *et al.*, 2012). However, except for hearing, which is based on a quantitative measurement (the length of the lagena; see subsequent discussion), our understanding of most senses are qualitative (comparisons of the relative sizes and/or volumes with other extinct and extant taxa). The REQ, olfactory acuity, hearing and balance can be calculated and interpreted from the cranial endocast of *Murusraptor*.

Reptile Encephalization Quotient (REQ). The volume of the cranial endocast is used to calculate the Encephalization Quotient (Jerison, 1973), which in turn is used to determine cognitive capabilities of extinct forms (Jerison, 1973; Franzosa, 2004; Larsson *et al.*, 2000). The Reptile Encephalization Quotient (Hurlburt, 1996) is an extension of the EQ based on brain-body relations in extant non-avian reptiles.

The complete volume of the cranial endocast of *Murusraptor* (including the olfactory bulbs) is approximately 148.2 ml (Tab. 1). Following Hurlburt *et al.* (2013), brain/endocranial volume ratios of 37% and 50% were used. The minimum calculated REQ of *Murusraptor* (using a volume of 37% of the total cranial endocast volume) is 1.33, whereas the maximum value (calculated using 50% of the cranial endocast volume) is 1.8 (Tab. 1). These values lie within the range of REQs calculated for allosauroid theropods (0.81–2.4), such as *Allosaurus*, *Giganotosaurus*, and *Sinraptor* (Tab. 1). This is about the range (1–2) calculated by Hopson (1977). When the complete volume (100%) of the cranial endocast of *Murusraptor* is used, the resulting REQ equals 3.43, which lies within the range of REQs (2.44–5.24) calculated for *Allosaurus* by Lautenschlager *et al.* (2012). In any case, in comparison with allosauroids, the REQ of *Murusraptor* is approximately 15% larger than that of *Giganotosaurus* and 35% larger than *Sinraptor*. It is sub-equal to the minimum calculated REQs for *Allosaurus* (Tab. 1). However, when compared to non-maniraptoran coelurosaurs, *Murusraptor* shows a REQ that is approximately 30–40% smaller than that of *Tyrannosaurus* (Hulburt *et al.*, 2013). This indicates that, although the morphological pattern of the cranial endocast of *Murusraptor* is more similar to that of non-maniraptoran coelurosaurs than to that of allosauroids, this similarity is not reflected by the REQ. This in turn suggests that the cognitive function for *Murusraptor* lay somewhere between those of allosauroids and tyrannosaurids.

Olfactory acuity. The olfactory bulbs and olfaction play an important role in the ecology of animals in general (activity timing, foraging, home range size, individual recognition, navigation, and reproduction; Zelenitsky *et al.*, 2009). The olfactory acuity depends both on the absolute size of the olfactory bulbs and their relative size compared to the cerebral hemispheres (see Zelenitsky *et al.*, 2009, 2011; and Material and Methods section). The olfactory bulbs of *Murusraptor* have a volume of 7 cm^3, which represents approximately 5% of the complete cranial endocast volume. The olfactory ratio (see Materials and Methods) of *Murusraptor* is approximately 45–50% (Tab. 1), which is similar to those of *Allosaurus* and Ceratosauria. Within theropods, the highest olfactory ratios are present in carcharodontosaurid allosauroids and tyrannosaurids (Zelenitsky *et al.*, 2009: tab. 1). When the log-transformed olfactory ratio (1.6) versus the log-transformed body mass (3.19) of *Murusraptor* are plotted in the graph published by Zelenitsky *et al.* (2011: fig. 2), the Argentinean taxon falls within the range of allosauroids. This suggests that there was nothing remarkable about the olfactory abilities of *Murusraptor* considering its body size. The olfactory acuity of an allosauroid is slightly higher than that of any ceratosaur, but lower than that of a tyrannosaurid. The latter have higher olfactory ratios than predicted for theropods of similar size, indicating a keener sense of smell (Zelenitsky *et al.*, 2009).

Hearing and balance. The vestibular region of the inner ear is associated with equilibrium and balance, whereas the lagenar region houses the sensory epithelium of the hearing organ. The length of the lagena is related to the length of the neuroepithelium of the basilar papilla and has been correlated with rough measures of auditory capability (behavioral importance of hearing) in extinct forms (Walsh *et al.*, 2009; Witmer and Ridgley, 2009 and references therein). Therefore, the short lagena present in *Murusraptor* suggests that airborne sounds were not particularly important to the behavior of this taxon. This is probably true for most theropod dinosaurs (Witmer and Ridgely, 2008), other than tyrannosaurids and therizinosaurs, which have long lagena (Lautenschlager *et al.*, 2012). Gleich *et al.* (2005) estimated low frequency hearing for *Allosaurus* (body mass equal to 1400 kg and lagena 8 mm long), with a high-frequency limit below 3 kHz. Because the estimated body mass and lagenar length in *Murusraptor* are only slightly larger than in

Allosaurus, a similar hearing range might be expected for the Argentinean taxon. In comparison, larger animals—such as tyrannosaurids—have larger lagena (Gleich *et al.*, 2005). This agrees with the acoustic consequences of extensive tympanic pneumaticity developed in this group, extending their ability to hear low frequency sounds (Witmer and Ridgely, 2009). The semicircular canals have also important neural links, coordinating eye movements and head turning (Spoor *et al.*, 2007, Witmer *et al.*, 2008, Witmer and Ridgely, 2009). Therefore, some inferences have been made on locomotor behavior (*e.g.*, bipedality), and the capability to perform fast movements of the head (Lautenschlager *et al.*, 2012 and references therein).

Sight and visual capabilities. Sight does not seem to be the most important sense in this taxon because the optic lobes are small enough that they are not differentiated in the cranial endocast. However, the large diameters of the optic tracts and optic nerves in *Murusraptor* and other theropods—including abelisaurids (Sampson and Witmer, 2007; Paulina-Carabajal 2011b; Paulina-Carabajal and Filippi, 2016) and carcharodontosaurids (Larsson et al., 2000; Paulina-Carabajal and Canale, 2010)—suggest sight was well-developed for at least oculomotor responses.

DISCUSSION

Braincase morphology and the phylogenetic placement of megaraptorans

The braincase and other skull bones of *Murusraptor* exhibit traits shared with non-maniraptoran Tetanurae. However, they also exhibit unique features. One of the most striking features of the skull roof of *Murusraptor* is the shape of the dorsal surface of the frontal, which is inclined lateroventrally from the midline, forming a perfect triangular cross section. This morphology has been not reported for any other theropod so far, and may represent an autapomorphy for this taxon. Other unique characters are a deep epipterygoid impression on the laterosphenoid (this impression is rarely observed in other theropods and indicates relatively restricted movements for the epipterygoid), separate canals for CN IV and the orbitocerebral vein that join distally to exit through a single foramen, and the presence of ossified ethmoidal elements (which do not contact the orbitosphenoids posteriorly so that there is an unnossified gap between the sphenethmoids and orbitosphenoids, a condition that has otherwise only been observed in *Sinraptor*; Paulina-Carabajal and Currie, 2012). Furthermore, braincase characters shared with non coelurosaur Tetanurae include the lack of a sagittal crest (the sagittal bar is low and wide), a low nuchal crest at the back of the skull roof (the nuchal crest does not rise above or is barely higher than the skull roof), a lack of pneumaticity besides that developed within the basicranium (basisphenoid recess, lateral tympanic recess), and an undivided internal metotic foramen (CNs IX–XI leave the endocranial cavity through a single foramen). Some characters are present in most theropods. For example, in *Murusraptor* the prefrontal is reduced (Coria and Currie, 2016), but almost excludes the frontal from the orbital margin as it extends backward along the orbital margin until it almost reaches the postorbital. In theropods, the lateral orbital region of the frontal is limited to the region between the postorbital and the prefrontal and/or lacrimal (depending on the posterior development of the lacrimal). In carcharodontosaurids, the palpebral closes the orbital margin by covering the frontal laterally (Coria and Currie, 2002a), whereas in abelisaurids the lacrimal contacts the postorbital so that it also excludes the frontal from the orbital margin. Minimum or restricted participation of the frontal in the orbital margin is also seen in *Sinraptor* (IVPP 10600), *Piveteausaurus* (Taquet and Welles, 1977), MCF-PVPH 320 (an isolated frontal, Paulina-Carabajal and Coria, 2015), and tyrannosaurids (Currie, 2003). In small theropods, the frontals participate largely in the orbital margins, whereas in mid to large-sized theropods the participation is reduced. However, variation in the degree of participation of the frontal in the orbital margin is clearly observed in the ontogeny of tyrannosaurids (Currie, 1987), and strongly suggests that the reduction in relative size of the frontal contribution of the orbital margin is size-related. In *Murusraptor*, the lacrimal does not project posterolaterally towards the prefrontal, but contacts the frontal anterior to the prefrontal. A similar situation is observed in tyrannosaurids, where the lacrimal contacts the frontal behind a reduced prefrontal (Currie, 2003: figs. 2, 7). This arrangement of the orbital elements seems to be a final stage of an evolutionary pathway in which the lacrimal extends posteriorly to restrict the prefrontal medially, but without contacting the frontal behind it. Unlike the condition in *Acrocanthosaurus* (Currie and

Carpenter, 2000) and *Allosaurus* (Madsen, 1976), the lacrimal tends not to contact the frontal behind the prefrontal. Porfiri *et al.* (2014) recognized some "tyrannosaurid" traits in a juvenile specimen of *Megaraptor*, and it is not surprising that initially *Murusraptor* was tentatively identified as a coelurosaur (Coria and Currie, 2002b).

An isolated theropod frontal, MCF-PVPH 320, from the Late Cretaceous of northern Patagonia (Paulina-Carabajal and Coria, 2015) shares several features with *Murusraptor*, suggesting that it is also a megaraptorid, although it appears to be a different taxon than *Megaraptor* (Porfiri *et al.*, 2014) and *Murusraptor*. These characters include a wide supratemporal fossa that covers more than the 50% of the length of the frontal (as in tyrannosaurids), the presence of a shallow pit and an alar projection on the dorsal surface of the postorbital process of the frontal (Figs. 5.1, 6.1), a short orbital vault, the presence of a triangular wedge of the parietals separating the frontals posteriorly (in *Murusraptor* the wedge is anteroventral, whereas in MCF-PVPH the wedge is anterodorsal, as in *Piatnitskysaurus*), a short and robust olfactory tract impression, and the greater relative size of the olfactory bulb impression (Figs. 5.2, 6.2).

Cranial endocast and sensorial capabilities. The particular morphology of the cranial endocast of *Murusraptor* shows closer similarities with non-maniraptoran coelurosaurs (including the forebrain-midbrain and midbrain-hindbrain angles, the relative length of the midbrain when compared to the length of the hindbrain, and the relative short olfactory tract) than with allosauroids and ceratosaurs (which have relatively elongate, narrow cranial endocasts, and relatively elongate midbrains). The midbrain region of *Murusraptor* is particularly short relative to other parts of the brain (the length of the midbrain—including the dorsal projection—is similar in length to the medulla oblongata), when compared to the markedly elongate midbrains of abelisaurids (*e.g.*, Sampson and Witmer, 2007; Paulina-Carabajal and Succar, 2015), the allosauroids *Allosaurus* (Sanders and Smith, 2005: fig. 3B; Witmer and Ridgely, 2009: fig. 4B), *Sinraptor* (Paulina-Carabajal and Currie, 2012), and carcharodontosaurids (Larsson, 2001; Franzosa and Rowe, 2005; Paulina-Carabajal and Canale, 2010), *Ceratosaurus* (Sanders and Smith, 2005: fig. 3A), and *Sinosaurus* (Carrano *et al.*, 2012; Xing *et al.*, 2014). This suggests a particular brain pattern for megaraptorids, which is different from that of known Allosauroidea and Ceratosauria. Unfortunately, the brain morphology is unknown for other megalosauroids with preserved braincases, including *Baryonyx* (BMNH R9951, Charig and Milner, 1986), *Dubreuillosaurus* (Allain, 2002, 2005), *Eustreptospondylus* (Huene, 1932), *Irritator* (SMNS 58022; Sues *et al.*, 2002), and *Piveteausaurus* (MNHN 1920-7, Taquet and Welles, 1977), which prevents further comparisons with representatives of this group.

However, even if the morphology of the brain of *Murusraptor* showed an intermediate stage between non-coelurosaur Tetanurae and non-maniraptoran coelurosaurs, the REQ of *Murusraptor* lies within that of allosauroids (Hulburt *et al.*, 2013; Tab. 1), suggesting that the neurosensorial capabilities in this taxon were not at the level of those calculated for tyrannosaurids.

CONCLUSIONS

This study presents the detailed description of the braincase anatomy and the first endocranial description for megaraptorids. The braincase anatomy of *Murusraptor* has a mosaic of plesiomorphic (basicranium) and derived (skull roof) characters. The brain morphology also suggests a mosaic of characters, sharing traits with both allosauroids and non-maniraptoran coelurosaurs. The first reconstruction of the endocranial anatomy of *Murusraptor* sheds light on the sensory adaptations of this Argentinean form. Differences with Allosauroidea and Ceratosauria suggest that megaraptorids had a characteristic brain morphology, more similar to that described for tyrannosaurids. However, neurosensorial capabilities based on brain morphology, REQs, and olfactory ratios of *Murusraptor* are more similar to those calculated for allosauroid theropods than to non-maniraptoran coelurosaurs. The anatomy of the olfactory bulb and the endosseous labyrinth of *Murusraptor* suggest that olfaction, hearing, and gaze stabilization were similar to those of allosaurids and ceratosaurs, the sense of olfaction being the most important for the Argentinean taxon.

AKNOWLEDGMENTS

R. Coria and A. Garrido (MCF), J. Calvo (CePALB), A. Kramarz (MACN), C. Muñoz (Museo Provincial "Carlos Ameghino"), J. Powell (PVL), J. Canale (Museo Municipal "Ernesto Bachmann"), L. Filippi (MAU), R. Martinez (PVL), R. Allain (MNHN), A. Milner (NHM), J. Gardner, and B. Strilisky (TMP), M. Carrano (USNM), R. Schoch (SMNS), and D. Brinkman (Yale Peabody Museum) permitted the study of the

specimens under their care. R. Coria is also thanked for allowing the first author to prepare and CT scan the braincase for her PhD Thesis. V. Arbour (at that time a U of A student) introduced APC to the use of the software Mimics; Dr. Z. Gasparini provided unfailing support to APC during the entire project. We thank O. Rauhut and S. Lautenschlager for their comments, which greatly improved the first version of this manuscript. CT scans of *Murusraptor* were made in Canada (2004) using grants from the Dinosaur Research Institute (to PJC), and the Jurassic Foundation (to APC). Support from PICT 2012-1425 (to APC) and NSERC (to PJC) are gratefully acknowledged.

REFERENCES

Ali, F., Zelenitsky, D.K., Therrien, F., and Weishampel, D.B. 2008. Homology of the ''ethmoid complex'' of tyrannosaurids and its implications for the reconstruction of the olfactory apparatus of non-avian theropods. *Journal of Vertebrate Paleontology* 28: 123–133.

Allain, R. 2002. Discovery of megalosaur (Dinosauria, Theropoda) in the Middle Bathonian of Normandy (France) and its implications for the phylogeny of basal Tetanurae. *Journal of Vertebrate Paleontology* 22: 548–563.

Allain, R. 2005. The postcranial anatomy of the megalosaur *Dubreuillosaurus valesdunensis* (Dinosauria, Theropoda) from the middle Jurassic of Normandy, France. *Journal of Vertebrate Paleontology* 25: 850–858.

Balanoff, A.M., Bever, G.S., and Ikejiri, T. 2010. The braincase of *Apatosaurus* (Dinosauria, Sauropoda) based on Computed Tomography of a new specimen with comments on variations and evolution in sauropod neuroanatomy. *American Museum Novitates* 3677: 1–29.

Baumel, J., and Witmer, L.M. 1993. Osteology. In: J. Baumel, A.S. King, J.E. Breazile, H.E. Evans, and J.C. Vanden (Eds.), *Handbook of Avian Anatomy: Nomina Anatomica Avium*. Publications of the Nuttall Ornithological Club, Cornell, p. 45–132.

Benson, R.B.J., Carrano, M.T., and Brusatte, S.L. 2010. A new clade of archaic large-bodied predatory dinosaurs (Theropoda: Allosauroidea) that survived to the latest Mesozoic. *Naturwissenschaften* 97: 71–78.

Bever, G.S., Brusatte, S.L., Balanoff, A.M., and Norell, M.A. 2011. Variation, variability, and the origin of the avian endocranium: insights from the anatomy of *Alioramus altai* (Theropoda: Tyrannosauroidea). *PLoS ONE* 6: e23393. doi:10.1371/journal.pone.0023393

Brochu, C. 2003. Osteology of *Tyrannosaurus rex*: Insights from a nearly complete skeleton and High-Resolution Computed Tomographic analysis of the skull. *Society of Vertebrate Paleontology Memoir* 7: 1–138; supplement to Journal of Vertebrate Paleontology 22(2).

Carrano, M.T., Benson, R.B.J., and Sampson, S.D. 2012. The phylogeny of Tetanurae (Dinosauria: Theropoda). *Journal of Systematic Palaeontology* 10: 211–300.

Cau, A., Dalla Vechia, F.M., and Fabbri, M. 2012. Evidence of a new carcharodontosaurid from the Upper Cretaceous of Morocco. *Acta Palaeontologica Polonica* 57: 661–665.

Charig, A.J., and Milner, A.C. 1986. *Baryonyx*, a remarkable new theropod dinosaur. *Nature* 324: 359–361.

Charig, A., and Milner, A.C. 1997. *Baryonyx walkeri*, a fish-eating dinosaur from the Wealden of Surrey. *Bulletin of the Natural History Museum of London (Geology series)* 53: 11–70.

Christiansen, P., and Fariña, R.A. 2004. Mass prediction in theropod dinosaurs. *Historical Biology* 16: 85–92.

Coria, R.A., and Currie, P.J. 2002a. The braincase of *Giganotosaurus carolinii* from the Upper Cretaceous of Argentina. *Journal of Vertebrate Paleontology* 22: 802–811.

Coria, R.A., and Currie, P.J. 2002b. Un gran terópodo celurosaurio en el Cretácico de Neuquén. *Ameghiniana, Suplemento Resúmenes* 39: 9R.

Coria, R.A., and Currie, P.J. 2016. A new megaraptoran dinosaur (Dinosauria, Theropoda, Megaraptoridae) from the Late Cretaceous of Patagonia. *PLoS ONE* 11: e0157973. doi:10.1371/journal.pone.0157973

Currie, P.J. 1987. Theropods of the Judith River Formation of Dinosaur Provincial Park, Alberta, Canada. *Tyrrell Museum of Palaeontology, Occasional Paper* 3: 52–60.

Currie, P.J. 1995. New information on the anatomy and relationships of *Dromaeosaurus albertensis* (Dinosauria: Theropoda). *Journal of Vertebrate Paleontology* 15: 576–591.

Currie, P.J. 1997. Braincase anatomy. In: P.J. Currie, and K. Padian (Eds.), *Encyclopedia of Dinosaurs*. Academic Press, New York, p. 81–84.

Currie, P.J. 2003. Cranial anatomy of tyrannosaurid dinosaurs from the Late Cretaceous of Alberta, Canada. *Acta Palaeontologica Polonica* 48: 191–226.

Currie, P.J., and Zhao, X.L. 1993a. A new carnosaur (Dinosauria, Theropoda) from the Jurassic of Xinjiang, People's Republic of China. *Canadian Journal of Earth Sciences* 30: 2037–2081.

Currie, P.J., and Zhao, X.L. 1993b. A new Troodontid (Dinosauria, Theropoda) braincase from the Dinosaur Formation. *Canadian Journal of Earth Sciences* 30: 2231–2247.

Currie, P.J., and Carpenter, K. 2000. A new specimen of *Acrocanthosaurus atokensis* (Dinosauria: Theropoda) from the Lower Cretaceous Antlers Formation (Lower Cretaceous, Aptian) of Oklahoma, USA. *Geodiversitas* 22: 207–246.

Currie, P.J., Hurum, J.H., and Sabath, K. 2003. Skull structure and evolution in tyrannosaurid dinosaurs. *Acta Palaeontologica Polonica* 48: 227–234.

Dufeau, D. 2011. [*The evolution of cranial pneumaticiy in Archosauria: patterns of paratympanic sinus development*. PhD Thesis, Faculty of the College of Arts and Sciences of Ohio University, Ohio, 175 p. Unpublished.].

Evans, D.C. 2005. New evidence on brain-endocranial cavity relationships in ornithischian dinosaurs. *Acta Palaeontologica Polonica* 50: 617–622.

Ezcurra, M.D. 2007. The cranial anatomy of the coelophysoid theropod *Zupaysaurus rougieri* from the Upper Triassic of Argentina. *Historical Biology* 19: 185–202.

Filippi, L., Méndez, A.H., Juárez Valieri, R.D., and Garrido, A.C. 2016. A new brachyrostran with hypertrophied axial structures reveals an unexpected radiation of latest Cretaceous abelisaurids. *Cretaceous Research* 61: 209–219.

Franzosa, J.W. 2004. [*Evolution of the brain in Theropoda (Dinosauria).* PhD Thesis, University of Texas, Austin, 357 p. Unpublished.].

Franzosa, J., and Rowe, T. 2005. Cranial endocast of the Cretaceous theropod dinosaur *Acrocanthosaurus atokensis*. *Journal of Vertebrate Paleontology* 25: 859–864.

Garrido, A.C. 2010. Estratigrafia del Grupo Neuquén, Cretácico Superior de la Cuenca Neuquina (Argentina): nueva propuesta de ordenamiento litoestratigrafico. *Revista Museo Argentino Ciencias Naturales* 12: 121–177.

Gleich, O., Dooling, R.J., and Manley, G.A. 2005. Audiogram, body mass, and basilar papilla length: correlations in birds and predictions for extinct archosaurs. *Naturwissenschaften* 92: 595–598.

Gow, C.E. 1990. Morphology and growth of the *Massospondylus* braincase (Dinosauria, Prosauropoda). *Palaeontologia Africana*

27: 59–75.

Gower, D.J. 2002. Braincase evolution in suchian archosaurs (Reptilia: Diapsida): evidence from the rauisuchian *Batrachotomus kupferzellensis*. *Zoological Journal of the Linnean Society* 136: 49–76.

Gower, D.J., and Weber, E. 1998. The braincase of *Euparkeria* and the evolutionary relationships of birds and crocodilians. *Biological Reviews* 73: 367–411.

Holliday, C.M. 2009. New insights into dinosaur jaw muscle anatomy. *The Anatomical Record* 292: 1246–1265.

Holliday, C.M., and Witmer, L.M. 2007. Archosaur adductor chamber evolution: integration of musculoskeletal and topological criteria in jaw muscle homology. *Journal of Morphology* 268: 457–484.

Hopson, J.A. 1977. Relative brain size and behavior in archosaurian reptiles. *Annual Review of Ecology, Evolution, and Systematics* 8: 429–448.

Hopson, J.A. 1979. Paleoneurology. In: C. Gans, R.G. Northcutt, and P. Ulinski (Eds.), *Biology of the Reptilia. Volume 9.* Academic Press, New York, p. 39–146.

Huene, F. von. 1932. Die fossile Reptil-Ordnung Saurischia, ihre Entwicklung und Geschichte. *Monographien zur Geologie und Palaeontologie* 4: 1–361.

Hurlburt, G.R. 1996. [*Relative brain size in recent and fossil amniotes: Determination and interpretation*. PhD Thesis, University of Toronto, Toronto. 250 p. Unpublished.].

Hurlburt, G.R., Ridgely, R.C., and Witmer, L.M. 2013. Relative size of brain and cerebrum in tyrannosaurid dinosaurs: an analysis using brain-endocast quantitative relationships in extant alligators. In: J.M. Parrish, E. Molnar, P.J. Currie, and E. Koppelhus (Eds.), *Tyrannosaurid Paleobiology*. Indiana University Press, Bloomington, p. 134–154.

Iordansky, N.N. 1973. The skull of the Crocodilia. In: C. Gans, and T. Parsons (Eds.), *Biology of the Reptilia. Volume 4*. Academic Press, New York, p. 201–262.

Jerison, H.J. 1973. *Evolution of the brain and intelligence*. Academic Press, New York, 482 p.

Knoll, F., Witmer, L.M., Ortega, F., Ridgely, R.C., and Schwarz-Wings, D. 2012. The braincase of the basal sauropod dinosaur *Spinophorosaurus* and 3D reconstructions of the cranial endocast and inner ear. *PLoS ONE.* doi:10.1371/journal.pone.0030060

Kurzanov, S.M. 1976. Braincase structure in the carnosaur *Itemirus* N. Gen. and some aspects of the cranial anatomy of dinosaurs. *Paleontological Journal* 3: 127–137.

Larsson, H.C.E. 2001. Endocranial anatomy of *Carcharodontosaurus saharicus* (Theropoda: Allosauroidea) and its implications for theropod brain evolution. In: D.H. Tanke, and K. Carpenter (Eds.), *Mesozoic vertebrate life*. Indiana University Press, Bloomington, p. 19–33.

Larsson, H.C.E., Sereno, P.C., and Wilson, J.A. 2000. Forebrain enlargement among nonavian theropod dinosaurs. *Journal of Vertebrate Paleontology* 20: 615–618.

Lautenschlager, S., Rayfield, E.J., Altangerel, P., Zanno, L.E., and Witmer, L.M. 2012. The endocranial anatomy of Therizinosauria and its implications for sensory and cognitive function. *PLoS ONE* 7: e52289. doi:10.1371/journal.pone.0052289

Leblanc, A. 1992. *Anatomy and imaging of the cranial nerves. A neuroanatomic method of investigation using magnetic resonance imaging (MRI) and computed tomography (CT).* Springer-Verlag, Berlin, 277 p.

Madsen, J.H. 1976. *Allosaurus fragilis:* A revised osteology. *Utah Geological and Mineral Survey Bulletin* 109: 1–163.

Martínez, R.N. 2009. *Adeopapposaurus mognai* gen. et sp. nov. (Dinosauria: Sauropodomorpha) with comments on adaptation of basal Sauropodomorpha. *Journal of Vertebrate Paleontology* 29: 142–164.

Mazzetta, G.V., Christiansen, P., and Fariña, R.A. 2004. Giants and bizarres: body size of some southern South American Cretaceous dinosaurs. *Historical Biology* 16: 71–86.

Miyashita, T., Arbour, V., Witmer, L.M., and Currie, P. 2011. The internal cranial morphology of an armoured dinosaur *Euoplocephalus* corroborated by X-ray computed tomographic reconstruction. *Journal of Anatomy* 219: 661–675.

Norman, D.B., and Faiers, T. 1996. On the first partial skull of an ankylosaurian dinosaur from the Lower Cretaceous of the Isle of Wight, southern England. *Geological Magazine* 133: 299–310.

Novas, F.E. 1998. *Megaraptor namunhuaiquii* gen. et. sp. nov., a large-clawed, Late Cretaceous theropod from Argentina. *Journal of Vertebrate Paleontology* 18: 4–9.

Novas, F.E. 2009. *The age of dinosaurs in South America*. Indiana University Press, Bloomington, 536 p.

Novas, F.E., Agnolin, F.L., Ezcurra, M.D., Porfiri, J., and Canale, J.I., 2013. Evolution of the carnivorous dinosaurs during the Cretaceous: the evidence from Patagonia. *Cretaceous Research* 45: 174–215.

Paulina-Carabajal, A. 2008. Abelisaurid theropod braincase pneumaticity: phylogenetic implications based on Argentinean specimens. *Ameghiniana, Suplemento Resúmenes* 45: 30R.

Paulina-Carabajal, A. 2009. [*El neurocráneo de los dinosaurios Theropoda de la Argentina. Osteología y sus implicancias filogenéticas*. Tesis Doctoral, Facultad de Ciencias Naturales y Museo, Universidad Nacional de La Plata, La Plata, 540 p. Unpublished.].

Paulina-Carabajal, A. 2011a. Braincases of abelisaurid theropods from the upper Cretaceous of north Patagonia. *Palaeontology* 54: 793–806.

Paulina-Carabajal, A. 2011b. The braincase anatomy of *Carnotaurus sastrei* (Theropoda: Abelisauridae) from the Upper Cretaceous of Patagonia. *Journal of Vertebrate Paleontology* 31: 378–386.

Paulina-Carabajal, A. 2012. Neuroanatomy of titanosaurid dinosaurs from the Upper Cretaceous of Patagonia, with comments on endocranial variability within Sauropoda. *The Anatomical Record* 295: 2141–2156.

Paulina-Carabajal, A. 2015. Guía para el estudio de la neuroanatomía de dinosaurios Saurischia, con énfasis en formas sudamericanas. *Publicación Electrónica de la Asociación Paleontológica Argentina* 15: 108–142.

Paulina-Carabajal, A., and Canale, J.I. 2010. Cranial endocast of the carcharodontosaurid theropod *Giganotosaurus carolinii. Neues Jahrbuch für Geologie und Paläontologie, Abhandlungen* 258: 249–256.

Paulina-Carabajal, A., and Currie, P.J. 2012. New information on the braincase and endocast of *Sinraptor dongi* (Theropoda: Allosauroidea): Ethmoidal region, endocranial anatomy and pneumaticity. *Vertebrata PalAsiatica* 50: 85–101.

Paulina-Carabajal, A., and Coria, R. 2015. An unusual theropod frontal from North Patagonia. *Alcheringa* 39: 514–518. doi:10.1080/03115518.2015.1042275

Paulina-Carabajal, A., and Succar, C. 2015. Endocranial morphology and inner ear of the theropod *Aucasaurus garridoi*. *Acta Palaeontologica Polonica* 60: 141–144.

Paulina-Carabajal, A., and Filippi, L. 2016. Neuroanatomy of the abelisaurid theropod *Viavenator*: The most complete reconstruction of brain and inner ear for a South American representative of the clade. *Ameghiniana, Suplemento Resúmenes* 53: 64.

Paulina-Carabajal, A., Canale, J.I., and Kundrát, M. 2015a. Nueva información sobre la neuroanatomía de *Giganotosaurus carolinii* usando tomografías computadas: morfología del oído interno. *Ameghiniana, Suplemento Resúmenes* 52: 32.

Paulina-Carabajal, A., Ezcurra, M.D., and Novas, F.E. 2015b. New information on the braincase and endocranial morphology of the late Triassic theropod *Zupaysaurus rougieri* using CT scans. *Ameghiniana, Suplemento Resúmenes* 52: 32–33.

Porfiri, J.D., Novas, F.E., Calvo, J.O., Agnolín, F.L., Ezcurra, M.D., and Cerda, A. 2014. Juvenile specimen of *Megaraptor* (Dinosauria, Theropoda) sheds light about tyrannosauroid radiation. *Cretaceous Research* 51: 35–55.

Raath, M.A. 1977. [*The anatomy of the Triassic theropod* Syntarsus rhodesiensis *(Saurischia: Podokesauridae) and a consideration of its biology*. Doctoral Thesis, Department of Zoology and Entomology, Rhodes University, Salisbury, 233 p. Unpublished.].

Rauhut, O.W.M. 2003. The interrelationships and evolution of basal theropod dinosaurs. *Special Papers in Palaeontology* 69: 1–213.

Rauhut, O.W.M. 2004. Braincase structure of the Middle Jurassic theropod dinosaur *Piatnitzkysaurus*. *Canadian Journal of Earth Sciences* 41: 1109–1122.

Rogers, S.W. 1998. Exploring dinosaur neuropaleobiology: Computed Tomography Scanning and analysis of an *Allosaurus fragilis* endocast. *Neuron* 21: 673–679.

Rogers, S.W. 1999. *Allosaurus*, crocodiles, and birds: evolutionary clues from spiral computed tomography of an endocast. *Anatomical Record* 257: 162–173.

Sampson, S.D., and Witmer, L.M. 2007. Craniofacial anatomy of *Majungasaurus crenatissimus* (Theropoda: Abelisauridae) from the Late Cretaceous of Madagascar. *Journal of Vertebrate Paleontology Memoir* 8: 32–102; supplement to Journal of Vertebrate Paleontology 27(2).

Sanders, K.R., and Smith, D.K. 2005. The endocranium of the theropod dinosaur *Ceratosaurus* studied with computed tomography. *Acta Palaeontologica Polonica* 50: 601–616.

Säve-Söderbergh, G. 1947. Notes on the brain-case in *Sphenodon* and certain Lacertilia. *Zoologiska Bidrag från Uppsala* 25: 489–516.

Spoor, F., Garland, T.H., Krovitz, G., Ryan, T.M., Silcox, M.T., and Walker, A. 2007. The primate semicircular canal system and locomotion. *Proceedings of the National Academy of Sciences* 104: 10808–10812.

Sues, H-D., Frey, E., Martill, D.M., and Scott, D.M. 2002. *Irritator challengeri*, a spinosaurid (Dinosauria: Theropoda) from the Lower Cretaceous of Brazil. *Journal of Vertebrate Paleontology* 22: 535–547.

Sues, H-D., Averianov, A., Ridgely, R.C., and Witmer, L.M. 2015. Titanosauria (Dinosauria, Sauropoda) from the Upper Cretaceous (Turonian) Bissekty Formation of Uzbekistan. *Journal of Vertebrate Paleontology* 35: e889145. doi: 10.1080/02724634.2014.889145

Taquet, P., and Welles, S.P. 1977. Redescription du crane de dinosaure Theropode de dives (Normandie). *Annales de Paléontologie (vertebres)* 63: 191–206.

Tumanova, T.A. 1987. The armored dinosaurs of Mongolia. *Transactions of the joint Soviet-Mongolian Paleontological Expedition* 32: 1–76.

Walsh, S.A., Barrett, P.M., Milner, A.C., Manley, G., and Witmer, L.M. 2009. Inner ear anatomy is a proxy for deducing auditory capability and behaviour in reptiles and birds. *Proceedings of the Royal Society B* 276: 1355–1360.

Witmer, L.M. 1997. The evolution of the antorbital cavity of archosaurs: a study in soft-tissue reconstruction in the fossil record with an analysis of the function of pneumaticity. *Journal of Vertebrate Paleontology Memoir* 3: 1–73; supplement to Journal of Vertebrate Paleontology 17(1).

Witmer, L.M., and Ridgely, R.C. 2008. Structure of the brain cavity and inner ear of the centrosaurine ceratopsid dinosaur *Pachyrhinosaurus* based on CT scanning and 3D visualization. In: P.J. Currie, W. Langston Jr., and D.H. Tanke (Eds.), *A new horned dinosaur from an Upper Cretaceous bone bed in Alberta*. Canada: NRC Research Press, Ontario, p. 117–144.

Witmer, L.M., and Ridgely, R.C. 2009. New insights into the brain, braincase, and ear region of tyrannosaurs (Dinosauria, Theropoda), with implications for sensory organization and behavior. *The Anatomical Record* 292: 1266–1296.

Witmer, L.M., Chatterjee, S., Franzosa, J., and Rowe, T. 2003. Neuroanatomy of flying reptiles and implications for flight, posture and behavior. *Nature* 425: 950–953.

Witmer, L.M., Ridgely, R.C., Dufeau, D.L., and Semones, M.C. 2008. Using CT to peer into the past: 3D visualization of the brain and ear regions of birds, crocodiles, and nonavian dinosaurs. In: H. Endo, and R. Frey (Eds.), *Anatomical imaging: towards a new morphology*. Springer-Verlag, Tokyo, p. 67–88.

Xing, L., Paulina-Carabajal, A., Currie, P.J., Xu, X., Dong, Z., and Burns, M. 2014. Braincase anatomy of the basal theropod *Sinosaurus,* from the lower Jurassic of China, studied using CT scans. *Acta Geologica Sinica* 88: 1653–1664.

Zelenitsky, D.K., Therrien, F., and Kobayashi, Y. 2009. Olfactory acuity in theropods: palaeobiological and evolutionary implications. *Proceedings of the Royal Society B* 276: 667–673.

Zelenitsky, D.K., Therrien, F., Ridgely, R.C., McGee, A.R., and Witmer, L.M. 2011. Evolution of olfaction in non-avian theropod dinosaurs and birds. *Proceedings of the Royal Society B* 278: 3625–3634.

doi: 10.5710/AMGH.25.03.2017.3062

Submitted: November 7th, 2016
Accepted: March 25th, 2017
Published online: March 28th, 2017